Enhancing associative learning in rats with a computationally designed training protocol

Xu O. Zhang; Yili Zhang; Claire E. Cho; Douglas S. Engelke; Paul Smolen; John H Byrne; Fabricio H. Do-Monte[#].

Department of Neurobiology and Anatomy, McGovern Medical School, The University of Texas Health Science Center at Houston, Houston, Texas 77030

#Corresponding author:

Fabricio H. Do Monte, DVM, PhD.

Phone: 713-500-5613

Email: fabricio.h.domonte@uth.tmc.edu

Abbreviated title: Enhancing learning with a computational model

Conflict of Interests: The authors declare no competing financial interests.

Keywords: Associative memory, fear conditioning, fear extinction, long-term potentiation, computational model, spaced learning.

Abstract

Learning requires the activation of protein kinases with distinct temporal dynamics. Nonassociative learning in *Aplysia* can be enhanced by a computationally designed learning protocol with intertrial intervals (ITIs) that maximize the interaction between fast-activated protein kinase A (PKA) and slow-activated extracellular signal-regulated kinase (ERK). We tested whether associative learning in mammals can be enhanced by an optimal learning protocol with irregular ITIs, predicted computationally to increase the overlap between PKA and ERK signaling in rat hippocampus. We simulated 1,000 training protocols with varying ITIs to predict this optimal protocol. With auditory fear conditioning, we found that male adult rats exposed to the optimal protocol with irregular ITIs exhibited impaired extinction memory acquisition within the session with a standard footshock intensity, and stronger fear memory retrieval and spontaneous recovery with a weaker footshock intensity, when compared to rats that received either massed or spaced conditioning protocols with the same number of footshocks and fixed ITIs. With fear extinction stimuli, we likewise observed that rats exposed to the optimal protocol showed improved extinction of contextual fear memory and attenuated spontaneous recovery, compared to rats that received standard extinction protocols. Immunohistochemistry confirmed that the optimal conditioning protocol increased phosphorylated cAMP responsive element binding (pCREB) protein levels in the dentate gyrus (DG) of the dorsal hippocampus, suggesting higher levels of LTP induction. These findings demonstrate the capacity of a behavioral intervention driven by a computational model of memory-related signaling pathways to enhance associative learning in mammals, and may provide greater insight into strategies to improve cognition in humans.

INTRODUCTION

Long-term memory (LTM) formation that lasts for days to years is believed to be mediated by synaptic plasticity including long-term potentiation (LTP) or its invertebrate analogue long-term facilitation (LTF), which require gene expression and protein synthesis (Martin et al., 2000; Kandel, 2001; Lynch, 2004; Alberini, 2009; Byrne and Hawkins, 2015). Studies in the last decades have investigated LTP/LTF and their underlying molecular processes as potential targets to enhance learning or restore memory deficits in laboratory animals. However, traditional interventions using systemic cognitive enhancers or intracerebral pharmacological manipulations (Sharif et al., 2021; Lauterborn et al., 2016; McGaugh and Petrinovich, 1965; Lynch et al., 2014; Fernandez et al., 2008) are either based on trial-and-error approaches in specific model systems or are highly invasive, preventing or hindering translation to humans.

An alternative approach to enhance learning and memory is to develop computational models to predict optimal learning protocols based on the intracellular molecular cascades that underlie LTM formation and LTP/LTF induction (Smolen et al., 2016; Smolen et al., 2020; Zhang et al., 2021). Previous studies have identified activation of PKA (Schacher et al., 1988; Goldsmith and Abrams, 1991; Muller and Carew, 1998) and of the mitogen-activated protein kinase (MAPK) isoform ERK (Martin et al., 1997; Sharma and Carew, 2004; Sharma et al., 2003) as essential cascades for LTF. These two pathways converge to phosphorylate transcriptional factors such as CREB, which subsequently induce expression of multiple plasticity-related genes during LTF induction (Dash et al., 1990; Bartsch et al., 1995; Liu et al., 2011; Guan et al., 2002; Mohamed et al., 2005). The observation that these two pathways exhibit distinct kinetics of activation

72 (Muller and Carew, 1998; Philips et al., 2007; Zhang et al., 2021), suggests that the
73 temporal activity patterns, and activation overlap, of these pathways may constitute an
74 important target to enhance associative learning. Accordingly, our previous study
75 demonstrated that a computationally designed protocol with irregular ITIs, predicted to
76 maximize the overlap of PKA and ERK activities, enhances LTF and nonassociative
77 learning, specifically long-term sensitization of the tail elicited siphon-withdrawal reflex in
78 *Aplysia* (Zhang et al., 2011).

79 Substantial similarities between molecular processes of LTF in invertebrates and
80 LTP in mammals make it plausible that strategies used to enhance LTF and
81 nonassociative learning in invertebrates could enhance LTP and associative learning in
82 mammals. PKA activation in rodent hippocampus and amygdala is required for LTP and
83 LTM (Schafe and LeDoux, 2000; Abel et al., 1997). Similarly, activation of ERK/MAPK
84 cascades and their cross-talk with PKA are required for CREB phosphorylation, induction
85 of plasticity-related genes, and LTP induction (Adams and Sweatt, 2002; Impey et al.,
86 1998; Bambah-Mukku et al., 2014; Tao et al., 1998). Although the temporal dynamics of
87 ERK and PKA activation in mammals differ from those in invertebrates (Roberson and
88 Sweatt, 1996; Vázquez et al., 2000; Wang et al., 2014), their common requirement for
89 LTP/LTM suggests that a protocol designed to maximize their activity overlap, with
90 irregular ITIs, may enhance memory formation in mammals.

91 Therefore, we tested if our invertebrate LTF model (Zhang et al., 2011) can be
92 adapted to computationally design an optimal associative learning protocol in mammals.
93 Because the majority of the above literature on LTP induction in mammals has focused
94 on fear conditioning experiments, we employed this well-established paradigm to

95 investigate associative learning (Johansen et al., 2011) and used empirical data from
96 the literature to model PKA and ERK dynamics in rat hippocampus (Wang et al., 2014;
97 Roberson and Sweatt, 1996; Vázquez et al., 2000), a critical brain region implicated in
98 the formation of associative memories in mammals (Milner et al., 1998; Mayes et al.,
99 2007; Nakazawa et al., 2002). We simulated 1,000 different training protocols with
100 varying ITIs to identify an optimal protocol with irregular ITIs that maximizes the overlap
101 of PKA and ERK activities and predicts the formation of stronger memory than training
102 protocols with the same number of stimuli and fixed ITIs. We then tested this optimal
103 protocol by using auditory fear conditioning and auditory fear extinction paradigms in
104 rats.
105

106 **RESULTS**

107 **A computational model based on PKA and ERK dynamics in rats identified an**
108 **optimal fear conditioning protocol**

109 The model in (Zhang et al., 2011) was adapted to simulate the dynamics of PKA and ERK
110 during the process of LTP induction in rat hippocampus (**Fig. 1A**). To the best of our
111 knowledge, hippocampus is the only rat brain region in which ERK dynamics has been
112 measured with a temporal resolution of minutes following a stimulus. In this model, the
113 stimulus (variable *Stim*) rapidly activates PKA via the cAMP pathway and slowly activates
114 ERK via the Raf-MEK pathway. The synergistic interaction between PKA and ERK
115 pathways is quantified by a variable *inducer*, which corresponds to the efficacy of the
116 stimulus in inducing LTP. ERK kinetics were described by differential equations (see
117 Methods) with parameter values reproducing empirical findings that ERK activity reaches

118 peak levels 15~20 min after BDNF treatment or tetanic stimuli in rat hippocampus acute
119 slices (Wang et al., 2014; Ajay and Bhalla, 2004). Equations describing PKA kinetics
120 simulated data showing that PKA is transiently activated within 2 min after LTP induction
121 in slices from rat hippocampus or within 5 min *in vivo* after spatial discrimination task
122 training (Roberson and Sweatt, 1996; Vázquez et al., 2000).

123 We simulated fear conditioning in rats, in which the pairing of a conditioned
124 stimulus (CS) with an unconditioned stimulus (US) is represented by *Stim*. The
125 conditioned responses are assumed to be proportional to the peak value of *inducer*. We
126 observed that a single CS-US pairing produced little overlap between PKA and ERK
127 pathways (**Fig. 1B1**). We then simulated 1,000 fear conditioning protocols, with 4 trials
128 and both fixed and irregular ITIs, to identify one predicted to have optimal ITIs for
129 triggering downstream gene activation. These simulations included a Short Conditioning
130 (SC) protocol with 4 trials and a fixed ITI of 270 s. We also simulated, as a reference
131 control, a Regular Conditioning (RC) protocol with 8 trials and the same ITI of 270 s.
132 These protocols respectively resemble previous protocols used for short and regular fear
133 conditioning in rats (Detert et al., 2008; Fanselow, 1980; Do-Monte et al., 2015). Our
134 simulations identified an optimal conditioning protocol with 4 trials and irregular ITIs of 8,
135 8, and 16 min (**Fig. 1B2-1B4**). Because the optimal protocol, like the SC protocol, has 4
136 trials, we term it Optimal Short Conditioning (OSC). Comparing OSC and SC in Fig. 1B3-
137 B4, both protocols produced pERK curves with similar peak levels (orange). However,
138 PKA activity induced by the last trial of OSC had a much larger overlap with the pERK
139 curve than did PKA induced by SC. Therefore, OSC induced a much higher peak level of

140 *inducer* (red). We therefore predicted the OSC protocol would produce stronger long-term

141 memory in rats than the standard SC protocol.

142

143

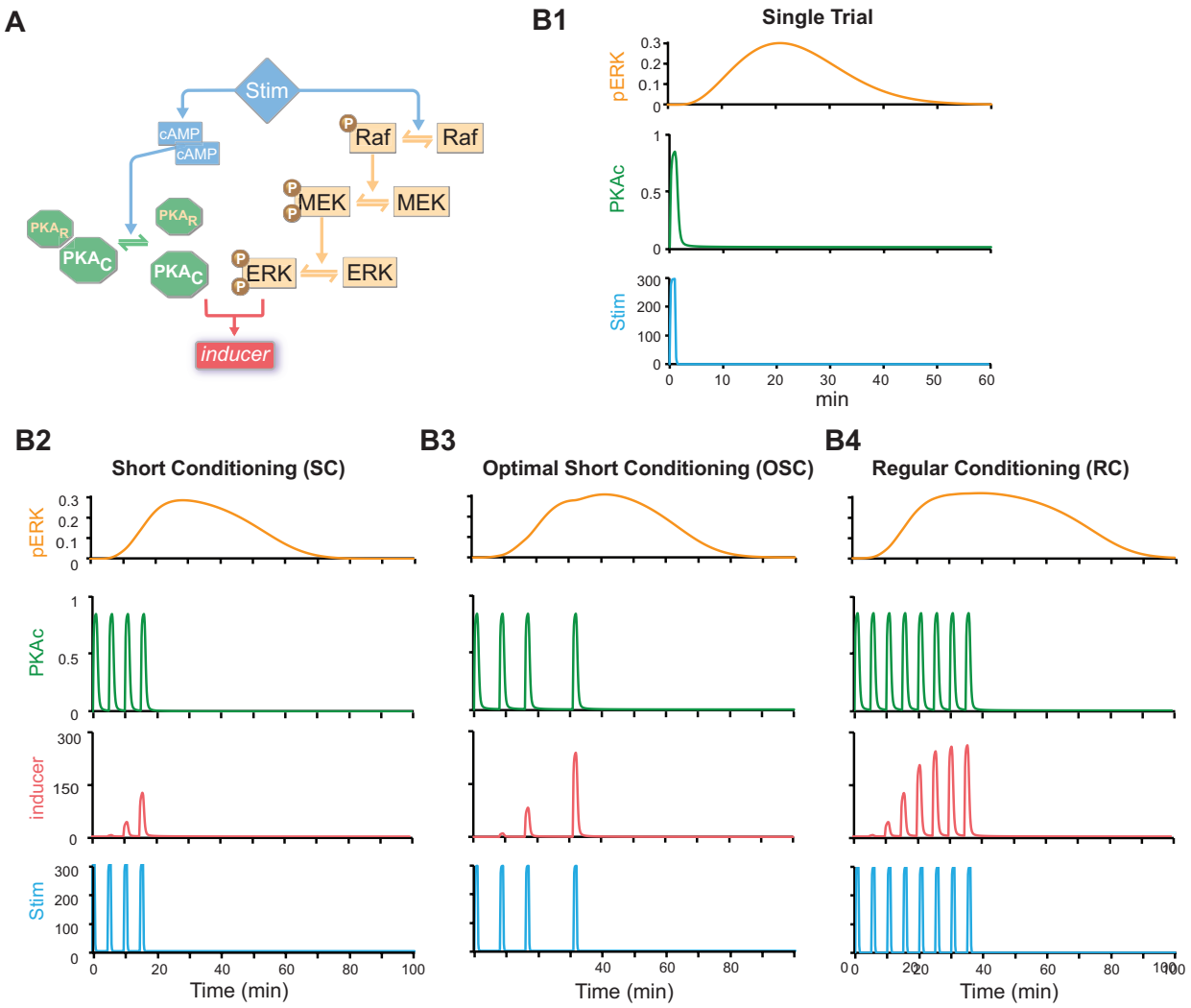

144

145 **Figure 1. Computational simulations of PKA and ERK pathways predict an optimal protocol**

146 **for fear conditioning. A**, Schematic of the model. Stimulus (*Stim*, μM) activates PKA via cAMP

147 and activates ERK via Raf-MEK. The variable *inducer* quantifies the PKA/ERK interaction (activity

148 overlap). **B1**, Simulated time courses of activated ERK (pERK, μM) and activated PKA (PKAc,

149 μM) in response to one trial of *Stim*. **B2**, Simulated time courses of pERK, PKAc, and *inducer* in

150 response to a 4-trial protocol with regular ITIs of 4.5 min (short conditioning, SC). **B3**, Simulated
151 time courses of pERK, PKAc, and *inducer* (nM) in response to a 4-trial protocol with
152 computationally designed intervals (optimal short conditioning, OSC).
153 **B4**, Simulated time courses of pERK, PKAc, and *inducer* (nM) in response to an 8-trial protocol
154 with regular ITIs of 4.5 min (regular conditioning, RC).
155

156 **The optimal short conditioning protocol induces an increase in fear memory when**
157 **compared to the standard short conditioning protocol**

158 To test if the OSC protocol could enhance associative learning in rats, we used a classical
159 auditory fear conditioning paradigm. Because the hippocampus is required for context
160 encoding during fear conditioning (Selden et al., 1991; Maren et al., 2013), we used two
161 different chambers (context A and context B) to assess the contribution of the context to
162 the auditory fear memory. The two contexts differed in size, floor texture, visual decoration
163 of the walls, and odor cues (**Fig. 2A**). On Day 0, rats were pre-exposed to context A for
164 20 min to familiarize with the chamber where fear conditioning took place in the following
165 day. Based on their baseline freezing and locomotor activity during the familiarization
166 session, rats were pre-assigned to one of the three experimental groups described above
167 in our simulations: Short Conditioning (SC), Optimal Short Conditioning (OSC), and
168 Regular Conditioning (RC). No significant difference was found among their baseline
169 freezing level (SC: 2.84%, OSC: 2.96%, RC: 3.05%, one-way ANOVA, $F_{(2, 37)} = 0.018$, P
170 $= 0.982$), average speed (SC: 0.025 m/s, OSC: 0.025 m/s, RC: 0.023 m/s, one-way
171 ANOVA, $F_{(2, 37)} = 0.062$, $P = 0.939$), and maximum speed (SC: 0.424 m/s, OSC: 0.446
172 m/s, RC: 0.439 m/s, one-way ANOVA, $F_{(2, 37)} = 0.044$, $P = 0.956$). On Day 1, rats were
173 placed into context A and exposed to one nonreinforced habituation tone (3 kHZ, 75 dB,

174 30 s) followed by distinct fear conditioning protocols (a total of 44 min duration, **Fig. 2B**).
175 The SC group received four presentations of CS (3 kHZ tone, 75 dB, 30 s) that co-
176 terminated with a US (footshock, 0.7 mA, 0.5 s) with ITIs of 270 s, and remained in the
177 chamber until the end of the session to equate the total context exposure time. The OSC
178 group received four similar CS-US pairings with ITIs of 8, 8, and 16 min. The RC group
179 received eight similar CS-US pairings with ITIs of 270 s. All groups reached high levels
180 of freezing (> 65%, **Fig. 2C**) and reduced locomotion at the end of the fear acquisition
181 session.

182 On Day 2, rats were placed in context B and given two CS presentations (ITI of
183 150 s, 7 min duration) in the absence of US to test the retrieval of tone-associated fear
184 memory in a novel context where no pre-tone freezing was observed in any of the groups
185 (Kruskal-Wallis's test. $H(2) = 3.887$, $P = 0.143$). Compared to the RC group, both SC and
186 OSC groups exhibited less freezing during the second CS presentation (Two-way
187 repeated measures (RM) ANOVA followed by Tukey's post-hoc test. $F_{(2, 37)} = 3.751$, $P =$
188 0.033; *a*, OSC vs. SC: $p = 0.527$; *b*, OSC vs. RC: $p = 0.029$; *c*, SC vs. RC: $p = 0.002$).
189 Yet, both RC and OSC groups showed reduced average speed during the retrieval test
190 compared to the SC group, suggesting generalized fear responses in a novel context (SC:
191 0.018 m/s, OSC: 0.013 m/s, RC: 0.01 m/s**;** One-way ANOVA followed by Tukey's post
192 hoc test. $F_{(2, 37)} = 10.87$, $P < 0.001$; *a*, OSC vs. SC: $p = 0.024$; *b*, OSC vs. RC: $p = 0.131$;
193 *c*, SC vs. RC: $p < 0.001$;).

194 On Day 3, rats were returned to context A for a retrieval and extinction training
195 session where they received twelve CS presentations (ITIs of 150 s, 37 min duration).
196 Prior to the first CS presentation, only the RC group showed a significantly higher pre-

197 tone freezing level (Kruskal-Wallis's test followed by Dunn's post hoc test. $H(2)$ = 13.93,
198 $P < 0.001$; *a*, OSC vs. SC, p > 0.999; *b*, OSC vs. RC, p = 0.020; *c*, SC vs. RC, p = 0.001),
199 suggesting a robust contextual fear memory. However, the three groups exhibited the
200 same levels of freezing during the first two CS presentations, suggesting that tone-evoked
201 fear retrieval was comparable among the groups (Two-way RM ANOVA. $F_{(22, 407)} = 1.169$,
202 $P = 0.271$). Nevertheless, a within session extinction analysis comparing the first four CSs
203 to the last four CSs revealed impaired extinction learning in the OSC and RC groups,
204 when compared to the SC group. This impairment in the acquisition of extinction in the
205 OSC and RC groups was characterized by sustained freezing levels within the session,
206 which differed from the SC group that showed reduced freezing levels from the first to the
207 last CS presentation (**Fig. 2D *left*;** Paired Student's t-test. *d*, OSC: $t_{13} = 0.869$, p = 0.400;
208 *e*, SC: $t_{11} = 4.191$, p = 0.001; *f*, RC: $t_{13} = 2.153$, p = 0.051**)**. Interestingly, the OSC group
209 exhibited persistent freezing levels during the extinction training session as indicated by
210 a reduced relative change in freezing from the beginning to the end of the session, when
211 compared to the SC group (**Fig. 2D *center*;** One-way ANOVA followed by Tukey's post-
212 hoc test. $F_{(2, 37)} = 3.315$, $P = 0.047$; *a*, OSC vs. SC: p = 0.037; *b*, OSC vs. RC: p = 0.487;
213 *c*, SC vs. RC: p = 0.320). In contrast, the SC group exhibited faster extinction acquisition
214 compared to the OSC and RC groups, as fewer CS presentations were required to
215 achieve 50% of reduction in the initial freezing levels (**Fig. 2D *right*;** Kruskal-Wallis's test
216 followed by Dunn's multiple comparisons test. $H(2)$ = 7.08, $P = 0.029$; *a*, OSC vs. SC: p
217 = 0.039; *b*, OSC vs. RC: p > 0.999; *c*, SC vs. RC: p = 0.095). Despite the persistent
218 freezing levels across the extinction training session observed in the OSC group, no
219 significant differences were found between the OSC and the SC groups during either the

220 extinction retrieval tests performed on Days 4 and 5 (Two-way RM ANOVA. context A:
221 $F_{(2, 37)}$ = 0.097, P = 0.907; context B: $F_{(2, 37)}$ = 2.984, P = 0.063) or the spontaneous
222 recovery tests performed on Days 29 and 30 (**Fig. 2C;** Two-way RM ANOVA followed by
223 Tukey's post hoc test. context A: $F_{(2, 37)}$ = 3.259, P = 0.049; RC vs. OSC: p = 0.027; RC
224 vs. SC: p = 0.038; OSC vs. SC: p = 0.999; context B: $F_{(2, 37)}$ = 0.774, P = 0.469). Taken
225 together, these data demonstrate that the computationally designed OSC protocol is able
226 to produce a modest enhancement of fear acquisition in rats, as indicated by reduced
227 locomotion speed in a new environment and stronger CS-evoked fear memory that is
228 more resistant to within-session extinction, although the enhancement did not persist
229 during the extinction retrieval and spontaneous recovery test.
230

231

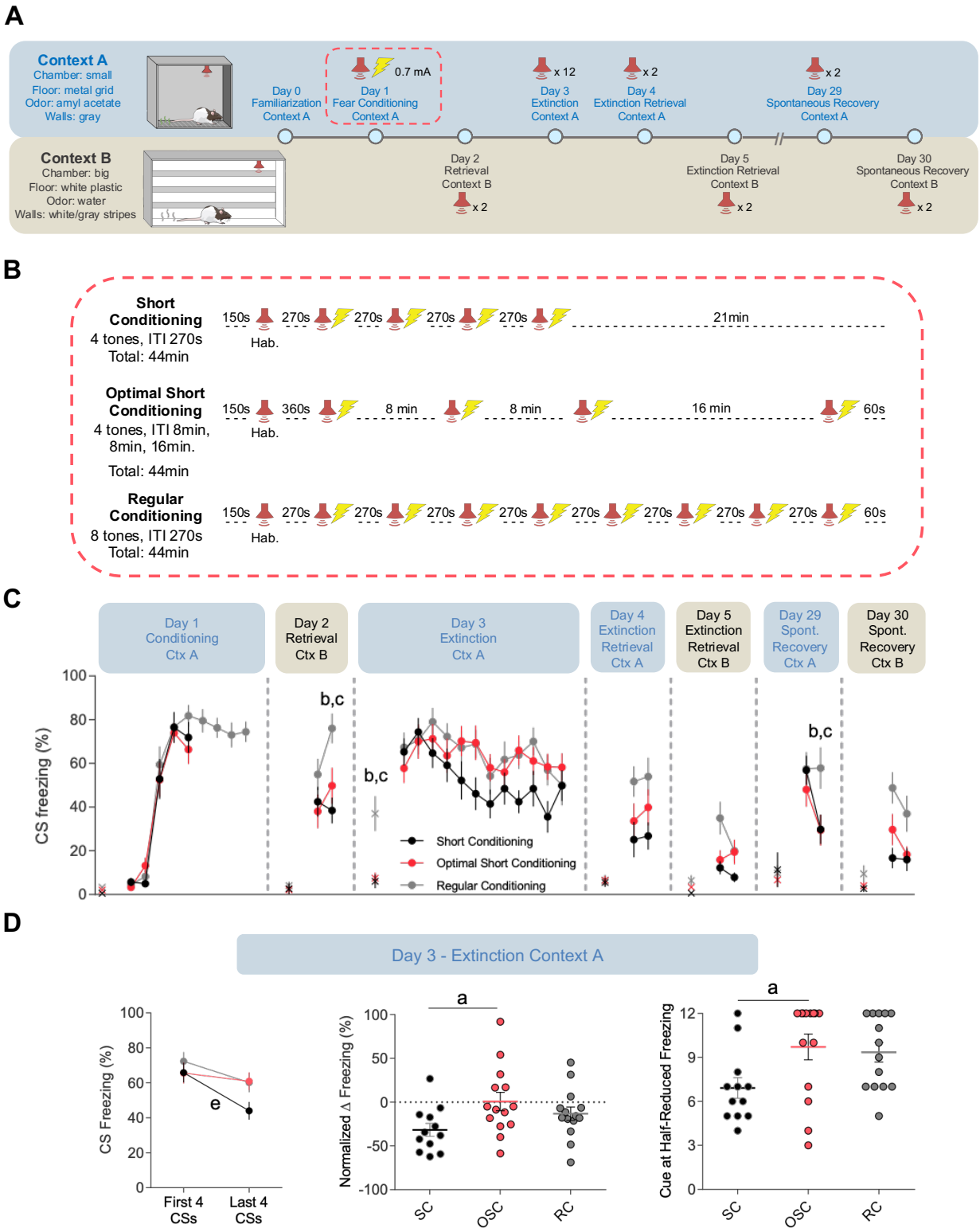
A
Context A
Chamber: small
Floor: metal grid
Odor: amyl acetate
Walls: gray
Day 0
Familiarization
Context A
0.7 mA
Day 1
Fear Conditioning
Context A
x 12
Day 3
Extinction
Context A
x 2
Day 4
Extinction Retrieval
Context A
x 2
Day 29
Spontaneous Recovery
Context A
Context B
Chamber: big
Floor: white plastic
Odor: water
Walls: white/gray stripes
Day 2
Retrieval
Context B
x 2
Day 5
Extinction Retrieval
Context B
x 2
Day 30
Spontaneous Recovery
Context B
x 2
B
Short Conditioning
4 tones, ITI 270s
Total: 44min
150s
270s
270s
270s
270s
21min
Hab.
Optimal Short Conditioning
4 tones, ITI 8min, 8min, 16min.
Total: 44min
150s
360s
8 min
8 min
16 min
60s
Hab.
Regular Conditioning
8 tones, ITI 270s
Total: 44min
150s
270s
270s
270s
270s
270s
270s
270s
270s
60s
Hab.
C
Day 1 Conditioning Ctx A
Day 2 Retrieval Ctx B
Day 3 Extinction Ctx A
Day 4 Extinction Retrieval Ctx A
Day 5 Extinction Retrieval Ctx B
Day 29 Spont. Recovery Ctx A
Day 30 Spont. Recovery Ctx B
CS freezing (%)
b,c
b,c
b,c
Short Conditioning
Optimal Short Conditioning
Regular Conditioning
D
Day 3 - Extinction Context A
CS Freezing (%)
e
First 4 CSs
Last 4 CSs
Normalized Δ Freezing (%)
a
SC
OSC
RC
Cue at Half-Reduced Freezing
a
SC
OSC
RC

232

233 **Figure 2. Computationally designed protocol partially enhanced fear conditioning in rats**.
234 **A,** Schematics of the enhanced fear conditioning experimental procedures. Top: tests that were
235 conducted in Context A. Bottom: tests that were conducted in Context B. **B,** Schematics of the
236 fear conditioning protocols for SC (n = 12), OSC (n = 14), and RC (n = 14) groups. Following a
237 habituation (Hab.) tone, rats received multiple trials of a CS (3 kHz tone, 30 s) that co-terminated
238 with a US (footshock, 0.7 mA, 0.5 s). **C,** Freezing levels during CS presentations of each group
239 across the experiment. Two-way Repeated-Measure ANOVA for each day followed by Tukey's
240 post hoc test. Letters *a, b*, and *c* indicate pairwise post hoc tests with $p < 0.05$: *a*, OSC vs. SC; *b*,
241 OSC vs. RC; *c*, SC vs. RC. '×' denotes the pre-tone freezing levels. **D,** OSC group is resistant to
242 extinction while SC group shows significantly more extinction. *Left*, freezing levels during the first
243 4 and last 4 CS presentations. Paired Student's t-test. Letter *e* indicates test with $p < 0.05$: SC,
244 Last 4 CS vs. First 4 CS. *Center*, normalized change of the freezing level during extinction, as
245 indicated by the difference of the freezing levels between last 4 and first 4 CS presentations as a
246 percentage of the freezing level of the first 4 CS presentations ((Last 4 CS – First 4 CS)/First 4
247 CS). One-way ANOVA followed by Tukey's post hoc test. * $p<0.05$. Letter *a* indicates pairwise
248 test with $p < 0.05$: OSC vs. SC. *Right*, the number of cues required to reach to a 50% reduction
249 of the original freezing level (average of freezing level during the first two cues). Kruskal-Wallis's
250 test followed by Dunn's multiple comparisons test. * $p<0.05$. Letter *a* indicates pairwise test with
251 $p < 0.05$: OSC vs. SC. Data shown here and in the next illustrations as mean ± SEM.
252

253 **The optimal short conditioning protocol induces stronger fear memory than a**
254 **spaced short conditioning protocol**

255 Spaced learning protocols result in stronger memories than massed learning protocols in
256 both humans (Cepeda et al., 2006; Raman et al., 2010) and rodents (Anderson et al.,
257 2008; Jiang et al., 2019; Scharf et al., 2002; but also see Cain et al., 2003). Thus, an

258 alternative explanation for the augmented fear memory observed in the OSC group in Fig.
259 2 could be simply trial-spacing effect, because our standard SC group used massed CS-
260 US pairings (i.e., briefer ITIs in SC than in OSC). In our simulations, both protocols
261 produced similar peak values of the pERK curves, but different degrees of overlap of PKA
262 and ERK activities, suggesting a way in which appropriately spaced protocols might
263 advantageously enhance overlap of kinase activities with distinct dynamics.

264 Indeed, there was a broad range of effective simulated 4-trial protocols (**Fig. 3**).
265 One protocol with relatively long, fixed ITIs of 11 min 10 s (i.e., 670 s) produced a nearly
266 identical peak level of *inducer* as the OSC protocol, and a higher peak level of *inducer*
267 than other protocols with fixed ITIs from 1 min to 21 min (**Fig. 3A, Fig. 4A1**). We termed
268 this protocol the Spaced Short Conditioning (SSC) protocol. We then examined the
269 effects of different stimulus intensities on predicting optimal training trials to address the
270 potential ceiling effect in these simulations. The 1,000 different protocols were re-
271 simulated with a reduced intensity of stimulus. Interestingly, the OSC protocol with
272 irregular ITIs of 8, 8, and 16 min still produced the greatest peak level of *inducer* (**Fig. 3B,**
273 **Fig. 4A2**). Equally interesting was that with weaker stimuli, the OSC protocol became
274 relatively more effective (higher peak *inducer*) than the SSC protocol. Therefore, we
275 predicted that the irregular intervals of the OSC may produce more effective conditioning
276 than the SSC protocol.

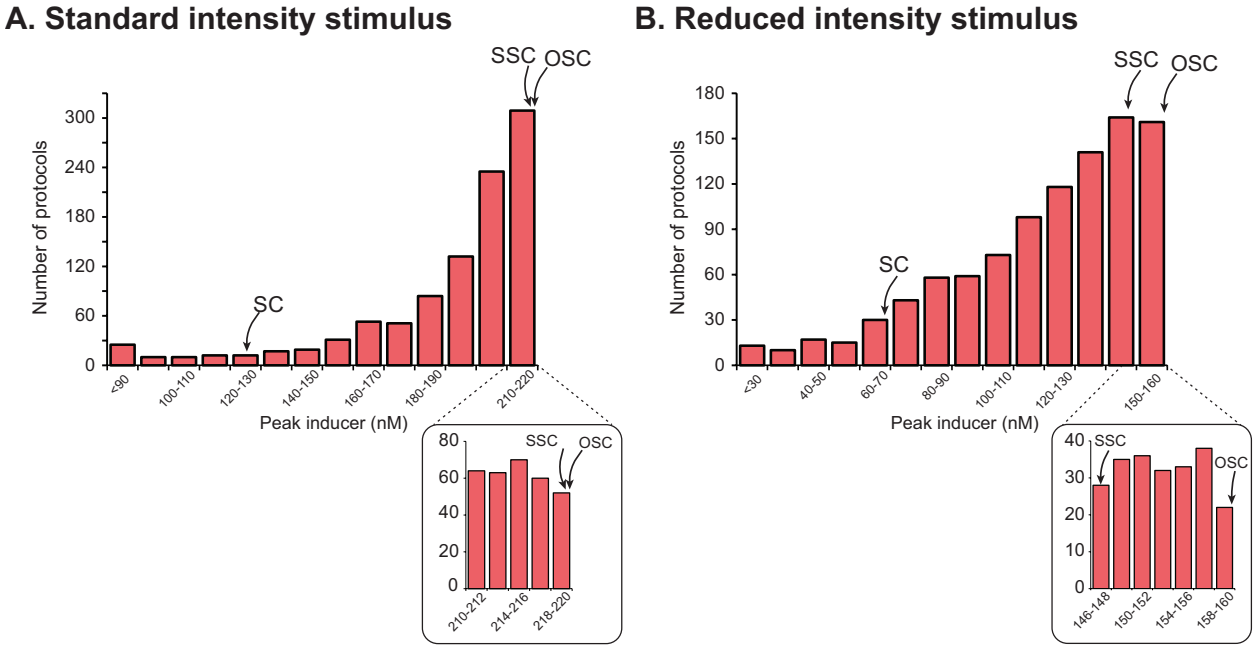

Figure 3. **Histogram of peak levels of *inducer* from 1,000 protocols. A**, Standard intensity stimulus (*Stim* = 300 μM). The range of peak levels of *inducer* (0 – 220 nM) was subdivided into 14 bins, and the number of simulations that produced a peak concentration of *inducer* in each subdivision was plotted. The arrows indicate which bins contained the peak concentrations produced by the short conditioning (SC), spaced short conditioning (SSC), and optimal short conditioning (OSC) protocols. **B,** Reduced intensity stimulus (*Stim* = 200 μM). The range of peak levels of *inducer* (0 – 160 nM) was subdivided into 14 bins, and the number of simulations that produced a peak concentration of *inducer* in each subdivision was plotted. Insets below the main plots illustrate in detail the difference in peak *inducer* for SSC *vs*. OSC, which is negligible in **A**.

To test this prediction, we empirically compared the SSC and OSC protocols using a reduced shock intensity (0.5 mA instead of the 0.7 mA used in Fig. 2) (**Fig. 4B**). Rats were pre-assigned to SSC or OSC groups based on their baseline freezing and locomotor

292 activity during the familiarization session. No significant difference was found between
293 their baseline freezing level (SSC: 3.72%, OSC: 5.21%, Unpaired Student's t-test, t_{16} =
294 0.988, P = 0.337), average speed (SSC: 0.016 m/s, OSC: 0.015 m/s, one-way ANOVA,
295 $F_{(2, 37)}$ = 0.062, P = 0.939), and maximum speed (RC: 0.439 m/s, SC: 0.424 m/s, OSC:
296 0.446 m/s, one-way ANOVA, $F_{(2, 37)}$ = 0.044, P = 0.956). During the fear acquisition, the
297 SSC group received 4 CS-US pairings with ITIs of 11 min 10 s, whereas the OSC group
298 was exposed to the same protocol as in Fig. 2 (*i.e.*, 4 CS-US pairings with ITIs of 8, 8,
299 and 16 min) (**Fig. 4C**). We found that the difference in the ITIs between the OSC and SSC
300 groups was sufficient to result in distinct levels of fear memory acquisition. Rats exposed
301 to OSC showed higher CS freezing levels during the third CS-US pairing of the fear
302 acquisition session (**Fig. 4D Day 1;** Two-way RM ANOVA followed by Tukey's planned
303 comparison. $F_{(4, 64)}$ = 1.550, P = 0.339; OSC vs. SSC: p = 0.019). In addition, fear memory
304 retrieval was increased when rats in the OSC group were returned to context A for an
305 extinction training session on Day 3, as indicated by higher freezing during the first two
306 CS presentations, compared to the SSC group (**Fig. 4D Inset;** Welch's t-test. $t_{12.43}$ = 2.227,
307 p = 0.045). Both OSC and SSC groups exhibited the same levels of freezing by the end
308 of the extinction training session (**Fig. 4D Day 3;** Two-way RM ANOVA followed by
309 Tukey's post hoc test. $F_{(11, 176)}$ = 2.997, P = 0.001; Tone 12, OSC vs. SSC: p > 0.999), as
310 well as during the extinction retrieval tests performed in context A (**Fig. 4D Day 4;** Two-
311 way RM ANOVA. $F_{(2, 37)}$ = 0.097, P = 0.907) or context B (**Fig. 4D Day 5;** Two-way RM
312 ANOVA. $F_{(2, 37)}$ = 2.984, P = 0.629). However, the OSC group showed greater
313 spontaneous recovery of fear memory in context A approximately 3 weeks later, as
314 indicated by higher freezing during the first CS presentation compared to SSC-trained

315 rats (**Fig. 4D Day 29;** Two-way RM ANOVA followed by Tukey's planned comparison. $F_{(2,}$
316 $_{32)}$ = 1.809, P = 0.180; OSC vs. SSC: p = 0.030). In summary, these data suggest that the
317 enhancement in fear memory acquisition observed with our computationally designed
318 OSC protocol cannot simply be attributed to a trial-spacing effect or differences in the
319 delay to remove the animals from the chamber, but it is rather associated with the
320 maximized overlap between PKA and ERK signaling.

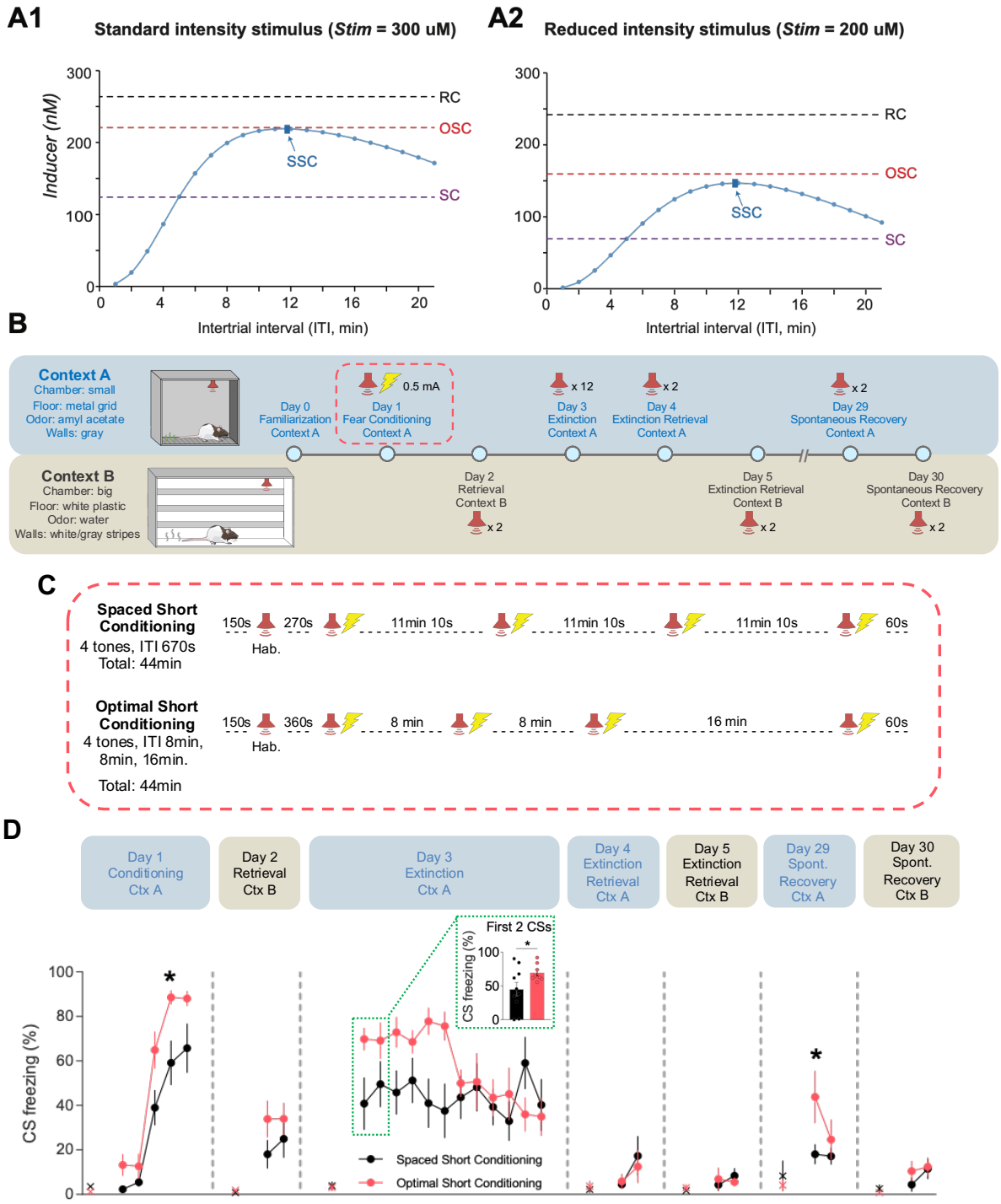

Figure 4. Optimal short conditioning protocol induced stronger fear memory than spaced short conditioning protocol in rats. A, *Inducer* peak levels from the RC, SC, and OSC protocols, compared to peak levels from short conditioning protocols of 4 trials with regular ITIs varying from

325 1 to 21 min, using standard intensity stimulus (**A1**) or reduced intensity stimulus (**A2**). The peak
326 *inducer* values of RC, SC, and OSC are labeled by dashed lines (black: RC; red: OSC; purple:
327 SC). The blue curve gives peak *inducer* values for the protocols with regular ITIs, and the curve
328 peaks at the dark blue dot and arrow, representing the SSC protocol with equal ITIs of 11 min
329 10s. **B,** Schematics of the fear conditioning procedures. Top: tests that were conducted in Context
330 A. Bottom: tests that were conducted in Context B. **C,** Schematics of the fear conditioning
331 protocols for SSC (n = 10, ITI = 11 min 10 s) and OSC (n = 8) groups. Following a habituation
332 (Hab.) tone, rats received 4 trials of a CS (3 kHz tone, 30 s) that co-terminated with a US
333 (footshock, 0.5 mA, 0.5 s). **D,** Freezing levels during CS presentations of each group across the
334 experiment; '×' denotes the pre-tone freezing levels. Two-way repeated-measure ANOVA for
335 each day followed by Tukey's pairwise post hoc test, * $p<0.05$. Inset: the average freezing level
336 during the first two CS presentations; Welch's t-test, * $p<0.05$.
337

338 **The optimal short conditioning protocol induces greater levels of phosphorylated**
339 **CREB in DG than a spaced short conditioning protocol**

340 The computational model predicts that the increased overlap of PKA and ERK activation
341 in OSC protocol leads to greater LTP induction (*inducer*) in rat hippocampus. One of the
342 mechanisms that may enhance LTP is increased convergence of the PKA and ERK
343 pathways to induce phosphorylation of CREB (Impey et al., 1998), a transcription factor
344 required for synaptic plasticity and LTP (Liu et al., 2011; Bourtchuladze et al., 1994; See
345 review by Kida, 2012). We therefore used immunohistochemistry to quantify the levels of
346 pCREB in rat dorsal hippocampus following fear conditioning in OSC versus SSC groups
347 (**Fig. 5A**), predicting the augmentation of fear conditioning in the OSC group would
348 correlate with increased pCREB. Rats were pre-assigned to OSC or SSC groups based

349 on their baseline freezing and locomotor activity during the familiarization session. No
350 significant difference was found between their baseline freezing level (SSC: 5.90%, OSC:
351 8.53%, Unpaired Student's t-test, $t_5 = 0.677$, $p = 0.528$), average speed (SSC: 0.014 m/s,
352 OSC: 0.015 m/s, Unpaired Student's t-test, $t_5 = 0.239$ $p = 0.820$), and maximum speed
353 (SSC: 0.272 m/s, OSC: 0.367 m/s, Unpaired Student's t-test, $t_5 = 1.697$, $p = 0.150$). During
354 the fear acquisition session, rats exposed to the OSC protocol showed freezing levels
355 similar to the SSC group during each CS presentation (**Fig. 5B**, Two-way RM ANOVA.
356 $F_{(4, 20)} = 0.848$, $P = 0.5112$.), but a significantly higher averaged freezing level across the
357 session (**Fig. 5B** Inset, Unpaired Welch's t-test, $t_{4.89} = 2.602$, $p = 0.049$). Approximately
358 15 min after the end of fear acquisition, rats were perfused and brains collected for
359 subsequent analyses. Immunohistochemistry revealed high levels of pCREB expression
360 across different hippocampal subfields in both OSC and SSC groups, with the highest
361 expression level being observed in the DG (**Fig. 5C**; Two-way ANOVA followed by
362 Tukey's post-hoc test. $F_{(3, 20)} = 4.533$, $P = 0.014$; CA1 vs. DG: $p < 0.001$; CA2 vs. DG: p
363 < 0.001; CA3 vs. DG: $p < 0.001$). Interestingly, rats exposed to the OSC protocol exhibited
364 increased pCREB expression in the DG when compared to the SSC group (**Fig. 5C-D;**
365 Two-way ANOVA followed by Bonferroni's post-hoc test. $F_{(3, 20)} = 4.533$, $P = 0.014$; OSC
366 vs. SSC: $p = 0.004$). Given that increased pCREB in the DG has been associated with
367 the induction efficiency of LTP in rodents (Davis et al., 2000), these data support the
368 hypothesis that the augmentation in fear memory acquisition observed with the OSC
369 protocol is mediated by higher levels of LTP induction in the rat hippocampus. Notably,
370 no group differences in pCREB expression were identified in other brain regions known
371 for being involved in fear memory acquisition such as the lateral, basal, and central nuclei

372 of the amygdala (Two-way ANOVA. $F_{(2, 15)} = 1.674$, $P = 0.22$) and the paraventricular

373 nucleus of the thalamus (PVT, unpaired Student's t-test, $t_5 = 1.697$, $p = 0.150$) (Fanselow

374 and LeDoux, 1999; Penzo et al., 2015).

375

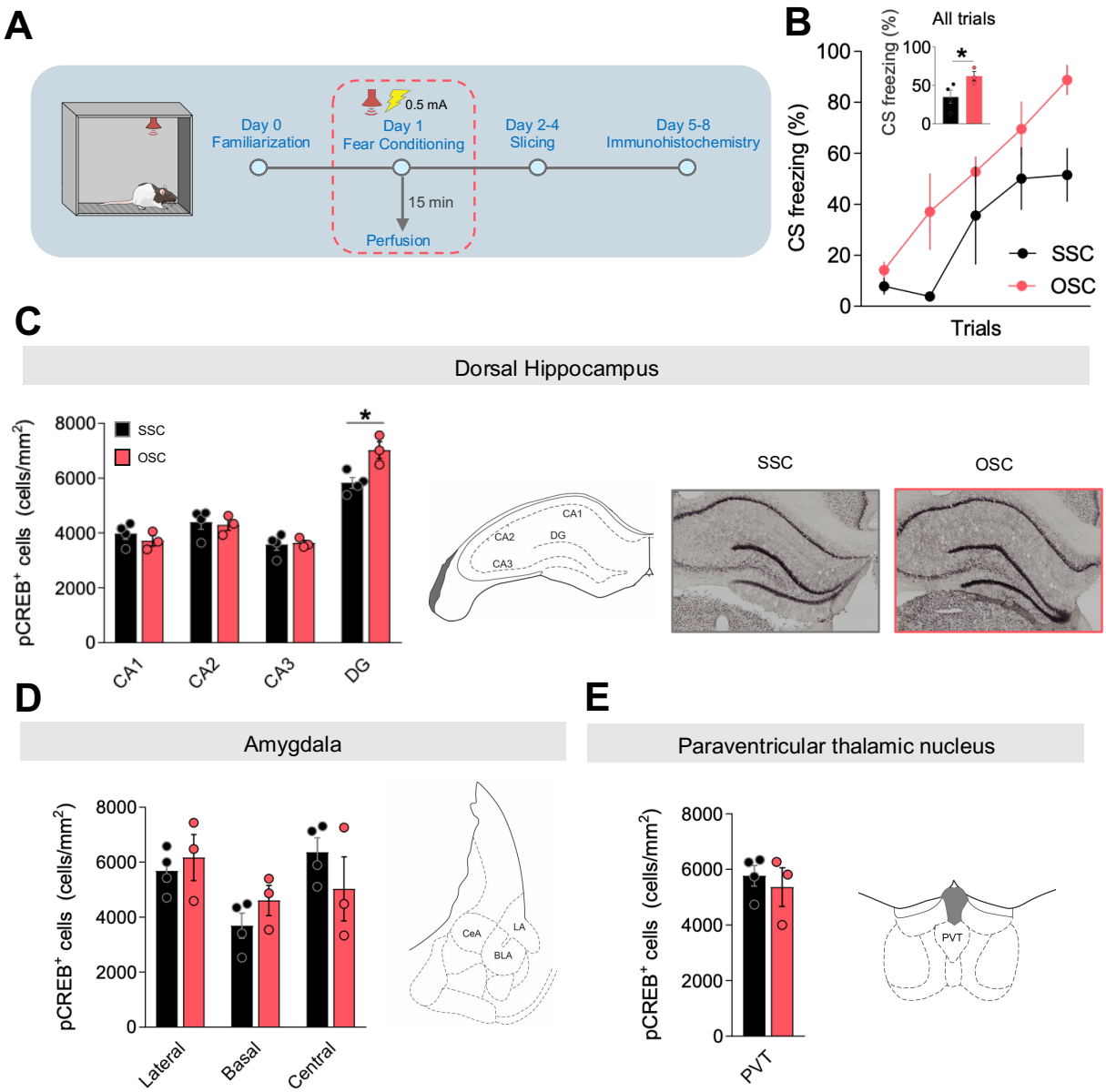

376

377 **Figure 5. Immunohistochemistry quantification of pCREB in hippocampus of rats exposed**

378 **to optimal versus spaced short conditioning protocols. A,** Schematic of the

379 immunohistochemistry procedure. **B,** Freezing levels during CS presentation for SSC (n = 4) and
380 OSC (n = 3) groups during fear conditioning; Two-way RM ANOVA followed by Bonferroni
381 correction. Inset, averaged freezing level for the 4 CS presentations; Welch's t-test, * p<0.05. **C,**
382 ***Left*,** Average pCREB density across hippocampal subfields for SSC (n = 4) and OSC (n = 3)
383 groups; Two-way ANOVA followed by Tukey's Bonferroni correction. *p < 0.05**;** ***Right***,
384 Representative images of pCREB immunostaining in distinct subfields of the dorsal hippocampus
385 (*left*) in the SSC group (*center*) and OSC group (*right*). **D,** Average pCREB density in the lateral
386 (LA), basolateral (BLA), and central (CeA) subregions of amygdala for SSC (n = 4) and OSC (n
387 = 3) groups; Two-way ANOVA followed by Tukey's Bonferroni correction. All p values > 0.05**; E**,
388 Average pCREB density in the paraventricular nucleus of the thalamus (PVT) for SSC (n = 4) and
389 OSC (n = 3) groups; unpaired Student's t-test, p = 0.150.
390

391 **The optimal short protocol also induced an enhancement in fear extinction**

392 Extinction is a new learning that temporarily inhibits the initial associative memory (de
393 Oliveira Alvares and Do-Monte, 2021; Quirk and Mueller, 2008). Because previous
394 studies suggest that fear extinction learning also relies on PKA and ERK signaling to
395 induce plasticity-related gene transcription (Flood et al., 1977; Szapiro et al., 2003;
396 Tronson et al., 2008), we predicted that the computationally designed protocol would also
397 enhance the acquisition of extinction, thereby suppressing the original fear memory (**Fig.**
398 **6A-B1**). We therefore used the OSC protocol with 4 trials and irregular ITIs of 8, 8, and
399 16 min as an Optimal Short Extinction (OSE) protocol (**Fig. 6B3**). We compared the OSE
400 protocol with a Regular Extinction (RE, **Fig. 6B4**) protocol using 12 trials and ITIs of 150
401 s, and a Short Extinction (SE, **Fig. 6B2**) protocol using 4 trials and the same ITIs of 150
402 s, which resemble previous protocols used for regular and short fear extinction in rats

403 (Santini et al., 2004; Holmes and Quirk, 2010; Do-Monte et al., 2015). Similar to the
404 simulation results for the conditioning protocols, the OSE protocol triggered higher peak
405 *inducer* than the SE protocol, and was comparable to the RE protocol (**Fig. 6B1-3**). We
406 thus predicted the OSE protocol would result in stronger extinction of fear memory than
407 the standard SE protocol.
408

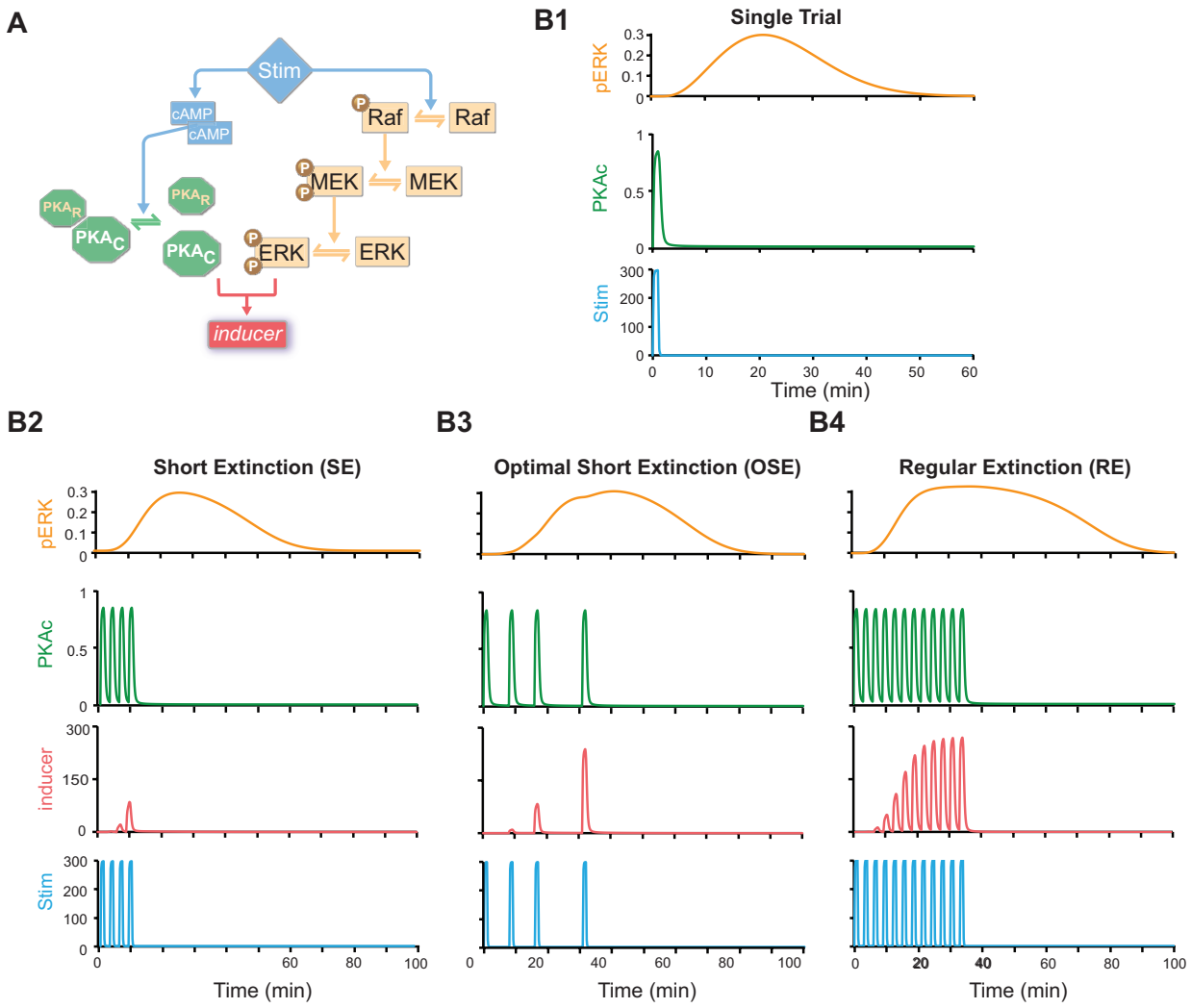

409

410 **Figure 6. Prediction of enhanced protocol for fear extinction. A**, Schematic of the model. **B1**,
411 Simulated time courses of activated ERK (pERK, μM) and activated PKA (PKAc, μM) in response
412 to one trial of *Stim* (μM). **B2**, Simulated time courses of pERK, PKAc, and *inducer* in response to

413 4-trial protocol with regular intervals of 2.5 min (short extinction, SE). **B3**, Simulated time courses
414 of pERK, PKAc, and *inducer* in response to 4-trial protocol with computationally designed intervals
415 (optimal short extinction, OSE). **B4**, Simulated time courses of pERK, PKAc, and *inducer* (nM) in
416 response to 12-trial protocol with regular intervals of 2.5 min (regular extinction, RE).
417
418 To test this prediction, we designed an experiment comparing the efficacy of
419 different extinction protocols (**Fig. 7A**). We used conditioned suppression of reward-
420 seeking behavior as an additional measure of fear memory because lever-press
421 suppression is more sensitive than freezing during fear extinction paradigms (Mast et al.,
422 1982; Sotres-Bayon et al., 2012). In addition, lever presses help to maintain a constant
423 level of activity so that freezing can be more reliably measured along the session (Quirk
424 et al., 2000). Since lever presses for reward are trained in a specific context, and
425 extinction memory is context-dependent (Podlesnik et al., 2017; Goode and Maren, 2014),
426 we used only one context in this experiment so that lever press suppression can be
427 consistently assessed across sessions and the extinction memory can be retrieved after
428 the extinction learning. Rats were initially trained to press a lever to receive sucrose
429 pellets in a variable interval schedule of 60 s. After 7 days of training, rats reached the
430 same levels of lever pressing (~10 presses/min) and locomotor activity.
431 On Day 8, rats underwent a fear conditioning session which included five
432 nonreinforced habituation tones (3 kHZ, 75 dB, 30 s duration) followed by seven CS-US
433 pairings (ITIs of 150 s, 37 min duration). We increased the footshock intensity from 0.7
434 mA to 1.0 mA, which resulted in stronger fear acquisition and consequently higher
435 freezing levels during the extinction session. This stimulus intensity also helped to avoid
436 a “floor effect” in the following tests. On Day 9, rats were pre-assigned to three

437 experimental groups based on their freezing and lever presses during the fear
438 conditioning session: Short Extinction (SE), Optimal Short Extinction (OSE), and Regular
439 Extinction (RE) (One-way ANOVA. $F_{(14, 231)} = 0.404$, $P = 0.973$). No significant difference
440 were observed among the groups' freezing levels (SE: 4.43%, OSE: 3.07%, RE: 3.20%,
441 Kruskal-Wallis's test $H(2) = 0.188$, $P = 0.910$), average speeds (SE: 0.036 m/s, OSE:
442 0.037 m/s, RE: 0.036 m/s, one-way ANOVA, $F_{(2, 33)} = 0.042$, $P = 0.958$), or lever presses
443 (SE: 9.64 presses/min, OSE: 9.603 presses/min, RE: 11.13 presses/min, one-way
444 ANOVA, $F_{(2, 33)} = 0.480$, $P = 0.622$). On Day 10, rats were returned to the same chamber
445 for a fear extinction session (39 min duration). The SE group received four CSs with ITIs
446 of 150 s and remained in the chamber until the end of the session; the OSE group
447 received four CSs with ITIs of 8, 8, and 16 min; and the RE group received twelve CSs
448 with ITIs of 150 s (**Fig. 7B**). At the end of the CS presentations, freezing levels reduced
449 from ~50% to ~20% in the RE group, whereas the SE and OSE groups maintained the
450 same levels of freezing throughout the four CSs (**Fig. 7C**, Day 9). Similarly, the RE group
451 showed a significant increase in lever presses (from 0.1 to 1.5 press/min) during the CS
452 presentations from the beginning to the end of the session, whereas CS lever presses
453 remained unaltered in the SE and OSE groups (**Fig. 7D *left*.** Paired Student's t-test; SE,
454 first 2 CS lever presses: 0 presses/min, last CS lever presses: 0.18 presses/min, t_{10} =
455 1.000, p = 0.341; OSE, first 2 CS lever presses: 0.46 presses/min, last CS lever presses:
456 1.23 presses/min, $t_{12} = 1.237$, p = 0.239; RE, first 2 CS lever presses: 0.08 presses/min,
457 last CS lever presses: 1.5 presses/min, $t_{11} = 2.837$, p = 0.016). However, the OSE group
458 showed a significant increase in lever presses during the 30-s periods that preceded the
459 CS presentations (pre-CS) when comparing the first two pre-CS periods to the last pre-

460 CS period of the extinction training session (**Fig. 7D *right***; Paired Student's t-test; SE: t_{10}
461 = 1.111, p = 0.293; OSE: t_{12} = 3.773, p = 0.003; RE: t_{11} = 0.994, p = 0.341), suggesting
462 enhanced within-session extinction of contextual fear memory (Morgan and LeDoux,
463 1995).

464 On Days 10 and 35, rats were returned to the same chamber and received two
465 CSs with an ITI of 150 s to test the strength of fear extinction memory during extinction
466 retrieval and spontaneous recovery tests, respectively. No significant difference in CS
467 freezing or CS lever presses were observed among the three groups during these tests
468 (**Fig. 7C, Day 10&35;** Two-way RM ANOVA. Day 10: Freezing, $F_{(2, 33)}$ = 0.207, P = 0.814;
469 Lever Presses, $F_{(2, 33)}$ = 0.069, P = 0.933; Day 35: Freezing, $F_{(2, 33)}$ = 0.535, P = 0.591;
470 Lever Presses, $F_{(2, 33)}$ = 1.085, P = 0.350). However, the OSE group showed increased
471 pre-CS lever pressing rate in the first pre-CS period (Two-way RM ANOVA followed by
472 Tukey's planned comparison, $F_{(2, 33)}$ = 2.897, P = 0.069; Tone 1, *a*, OSE vs. SE, p = 0.005;
473 *b*, OSE vs. RE, p = 0.025; *c*, SE vs. RE, p = 0.791) and also upon averaging the two pre-
474 CS periods during the spontaneous recovery test (**Fig. 7E *right***; Kruskal-Wallis's test
475 followed by Dunn's post hoc test. $H(2)$ = 6.414, P = 0.041; a: OSE vs. SE, p = 0.035; b:
476 OSE vs. RE, p = 0.531; c: SE vs. RE, p = 0.709), when compared to the SE and RE
477 groups on day 35. These results suggest that, although the tone-associated memory was
478 similar among the groups, the computationally designed OSE protocol was able to
479 enhance the extinction of contextual fear memory, as indicated by enhanced within-
480 session extinction of conditioned suppression and by reduced conditioned suppression
481 approximately 3 weeks after the extinction training session.

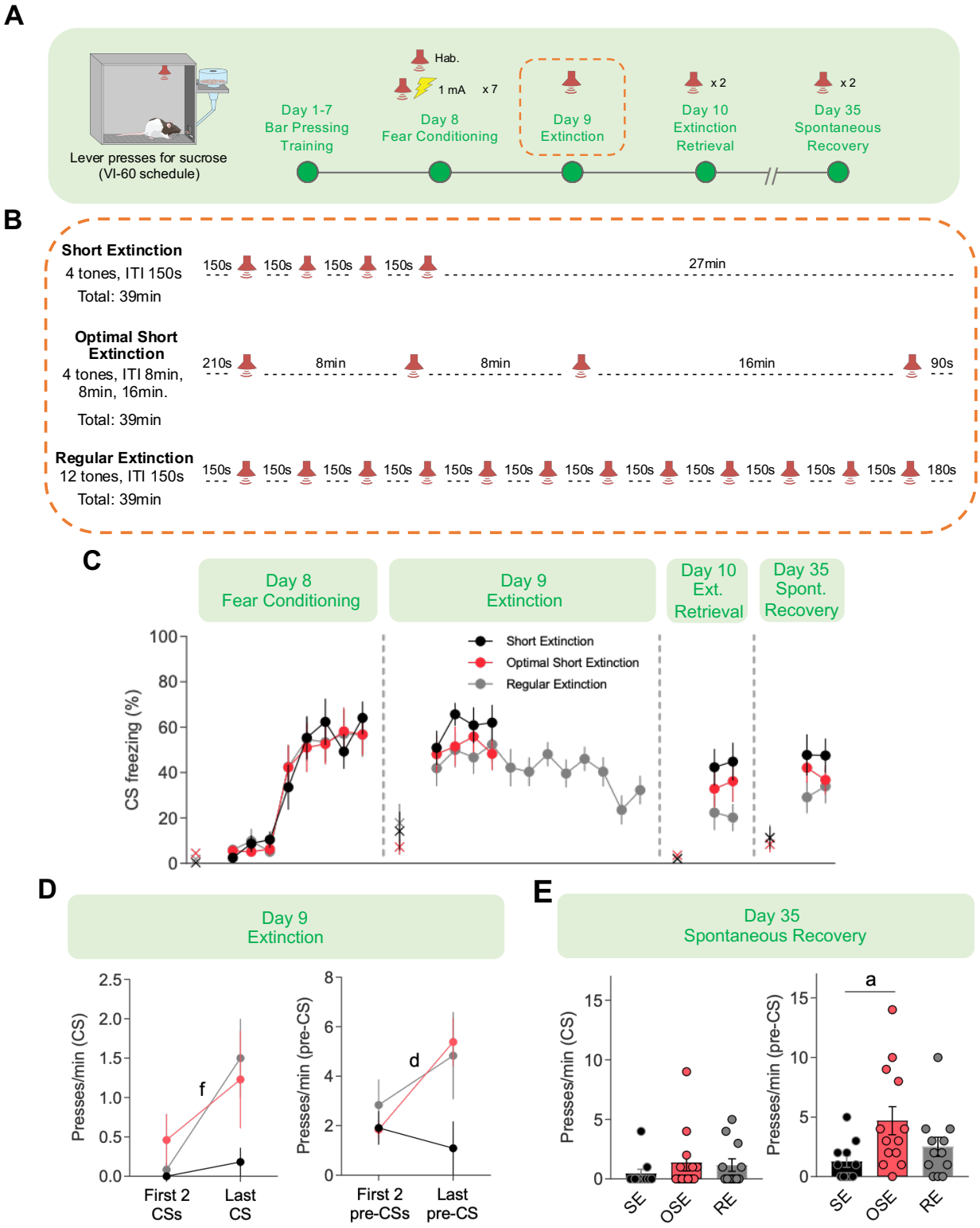

Figure 7. The computationally designed protocol partially enhanced fear extinction in rats. **A.** Schematic of the enhanced fear extinction experimental procedures. Rats were trained to

485 constantly press a lever to retrieve sucrose pellets in a variable interval 60 (VI60) schedule, where
486 the average interval between each sucrose delivery is 60 s. **B,** Schematics of the fear extinction
487 protocols for SE (n = 11), OSE (n = 13), and FE (n = 12) groups, during which rats received
488 multiple trials of a CS (3 kHz tone, 30 s). **C,** Freezing levels during CS presentations of each
489 group across the experiment. No significant difference between groups was found by Two-way
490 RM ANOVA. '×' denotes the pre-tone freezing levels. **D,** Lever press rates during the first two and
491 the last CS presentation (*left*) or the 30 s before the first two and the last CS presentation (pre-
492 CS period) of each group. OSE group shows significant increase of pre-CS lever presses
493 comparing the last CS presentation to the average lever press rate of the first two CS
494 presentations. Paired Student's t-test. Letters *f* and *d* indicate tests with $p < 0.05$: *f*, RE, Last CS
495 vs. First 2 CS; *d*, OSE, Last pre-CS vs. First 2 pre-CS. **E,** OSE group shows higher lever presses
496 during pre-CS period compared to SE group in spontaneous recovery test. No difference was
497 found for the CS lever presses among the three groups ($H(2) = 2.102$, $P = 0.349$). Kruskal-
498 Wallis's test followed by Dunn's post hoc test. Letter *a* indicates pairwise comparison with
499 *p<0.05: OSE vs. SE.
500

501 **DISCUSSION**

502 A computationally designed protocol that maximizes the interaction between PKA and
503 ERK pathways enhances LTF and nonassociative learning in *Aplysia* (Zhang et al., 2011).
504 Here, we extended the feasibility of this computational approach to associative learning
505 in mammals by adapting the simplified mathematical model used in *Aplysia* to simulate
506 the dynamics of PKA and ERK in rat hippocampus based on the available empirical data
507 in the literature (Wang et al., 2014; Roberson and Sweatt, 1996; Vázquez et al., 2000).
508 After simulating 1,000 different training protocols of auditory fear conditioning, we
509 identified an optimal protocol with irregular ITIs which resulted in extinction-resistant

510 memory formation using a standard footshock intensity, or stronger fear acquisition using
511 a weaker footshock intensity in rats, as compared to either massed or spaced training
512 protocols with the same number of trials, fixed ITIs, and comparable footshock intensities.
513 Immunohistochemistry demonstrated that the augmented fear memory induced by the
514 optimal protocol was associated with increased expression levels of pCREB in the DG
515 subfield of the dorsal hippocampus. Using a separate fear extinction paradigm, we also
516 showed that the optimal learning protocol was sufficient to induce a modest enhancement
517 in extinction memory in rats characterized by reduced expression of contextual fear, when
518 compared to regular or short extinction protocols with equal ITIs. Our results demonstrate
519 the power of a simplified model of intracellular signaling cascades in guiding associative
520 learning across species, attesting the essential role of the interaction between PKA and
521 ERK pathways in both nonassociative and associative learning.

522 Training protocols using spaced ITIs result in stronger memory acquisition than
523 those using standard massed ITIs, a well-established phenomenon described as the
524 "spacing effect" (see review by Smolen et al., 2016). Data demonstrating this effect in
525 animals and humans illustrate the relationship between the duration of the ITIs and the
526 strength of memory formation as an inverted-U-shape curve (Barela, 1999; Verkoeijen et
527 al., 2005), consistent with our simulated results (**Fig. 4A**). Previous findings have
528 attributed this spacing effect to the different efficacy of massed vs. spaced protocols in
529 inducing LTP/LTF through plasticity-related signaling. For example, spaced training
530 protocols in rodents lead to increased activation of ERK (Ajay and Bhalla, 2007), followed
531 by CREB phosphorylation and the expression of downstream genes, which have not been
532 reported following massed training protocols in the same species (Genoux et al., 2002).

533 A computational model based on slice electrophysiology from rat hippocampal data has
534 found that the peak of ERK activation aligns with the optimal ITI for LTP induction (Ajay
535 and Bhalla, 2004). Although that study provided a possible mechanism for the trial-
536 spacing effect and a potential approach to identify more effective protocols for associative
537 learning, it relied on fixed ITIs that are not necessarily the optimal intervals to induce
538 synaptic plasticity and LTM. In fact, our simulations predicted that an optimal protocol with
539 irregular ITIs was superior to most spaced protocols with the same number of trials and
540 equal ITIs. In the fear conditioning experiment, this optimal protocol induced stronger and
541 persistent fear memory in rats, when compared to a spaced protocol that had been
542 predicted to be the most effective among protocols with equal ITIs. These results suggest
543 that the spacing effect in mammals can be at least partially explained by enhanced
544 overlap between PKA and ERK pathways, which are critical for CREB activation (Impey
545 et al., 1998). More importantly, our findings demonstrate that protocols that include
546 irregular ITIs can be a better approach to enhance learning than previous protocols using
547 equal ITIs. Although the activation levels of PKA and ERK may vary across different brain
548 subregions and behavioral protocols, the chronological order of activation for these two
549 intracellular molecules is very well-conserved across species with a PKA peak preceding
550 the nuclear translocation of ERK and the subsequent activation of CREB in Aplysia
551 (Muller and Carew, 1998; Philips et al., 2007), mice (Impey et al., 1998), and rats (Vossler
552 et al., 1997; Roberson et al., 1999; Ahmed and Frey, 2005). Therefore, this evolutionarily-
553 conserved sequence of molecular events provides strong support for our model.

554 The enhanced performance of our optimal protocol (OSC) compared to a spaced
555 protocol (SSC) during fear conditioning appears constrained by the intensity of stimuli.

556 The model predicts higher performance for OSC when weak stimuli are used, but
557 comparable performance when strong stimuli are used (**Fig. 4A**). Drawing a line to
558 distinguish weak and strong footshock intensities is not straightforward because the
559 relationship between fear memory and footshock intensity is neither monotonic nor linear
560 (Davis and Astrachan, 1978). Nevertheless, we observed clear differences in the efficacy
561 of the optimal fear conditioning protocol when using footshocks of different intensities.
562 When we compared the optimal short conditioning protocol to a massed short
563 conditioning protocol using a standard footshock intensity (0.7 mA, **Fig. 2**) commonly
564 used in previous studies (Abel et al., 1997), we found only small differences in the
565 conditioned responses (CS freezing) between the two protocols. However, when we used
566 a lower footshock intensity (0.5 mA, **Fig. 4**) to compare the optimal short conditioning
567 protocol to a spaced short conditioning protocol, we found a significant increase in CS
568 freezing in the OSC group during fear acquisition, retrieval, and spontaneous recovery
569 tests. Considering the robustness of the spacing effect, it is possible that differences
570 between the OSC and the massed SC groups at the higher footshock intensity were in
571 part masked by a "ceiling effect". Alternatively, previous studies in rats have demonstrated
572 that the hippocampus is required for tone-evoked fear memory when a weak (0.4 mA) but
573 not a strong (0.9 mA) footshock is used (Quinn et al., 2008), which could also explain the
574 differences we observed at the two intensities. Either way, our data suggest that our
575 approach could be more beneficial for learning protocols relying on relatively weak stimuli.
576 Additional studies need to be conducted to understand the mechanism by which the
577 intensity of stimuli governs the enhanced performance of protocols with irregular ITIs
578 compared to protocols with fixed ITIs.

579 The association between the CS and US is primarily mediated by the lateral
580 amygdala where LTP induces enhanced CS responses (see review by Maren, 2005;
581 Johansen et al., 2011). Nevertheless, another important and distinguishable component
582 of fear memory formation is the context in which the association has occurred. In the fear
583 conditioning experiment, enhanced CS freezing was only observed in the same context
584 where fear conditioning took place, suggesting that the memory facilitation effect induced
585 by our optimal protocol is context dependent. Similarly, in the fear extinction experiment,
586 enhancement by the optimal protocol was only observed during the pre-CS lever pressing,
587 a more sensitive index of contextual fear memory during extinction and spontaneous
588 recovery (Morgan and LeDoux, 1995; Padilla-Coreano et al., 2012; Woods and Bouton,
589 2008; Sotres-Bayon et al., 2012; Mast et al., 1982). These results are consistent with
590 current empirical data from rat hippocampus, on which our model is based. The
591 hippocampus plays major roles in context encoding during fear conditioning, fear
592 extinction, and the time-dependent reappearance of fear following extinction training (*i.e.*,
593 spontaneous recovery) (see reviews by Maren et al., 2013; Bouton et al., 2021).
594 Accordingly, our immunohistochemical results showed greater pCREB expression
595 specifically in the DG of the dorsal hippocampus, a region implicated in the acquisition
596 and extinction of contextual fear memory (Kheirbek et al., 2013; Bernier et al., 2017).
597 Increasing CREB expression in DG neurons using a viral approach has been
598 demonstrated to improve contextual fear acquisition (Restivo et al., 2009), whereas
599 chemogenetically or optogenetically inactivating DG neurons that overexpress CREB
600 disrupts contextual fear retrieval (Park et al., 2016).

601 Another hippocampal subregion implicated in contextual fear is the CA1 (Hunsaker
602 and Kesner, 2008). Although the OSC and SSC groups displayed similar levels of pCREB
603 expression in CA1, the single post-training time point we used does not suffice to rule out
604 the possibility of distinct pCREB dynamics in CA1 compared to DG. Indeed, prior reports
605 have shown that CA1 pCREB expression peaks at 30 min and disappears at 90 min
606 following fear conditioning (Sindreu et al., 2007; Chaaya et al., 2019), a timeframe that
607 differs from the 15 min post-training interval we used to detect group differences in
608 pCREB expression. Further experiments comparing distinct post-training intervals may
609 better reveal the dynamics of pCREB expression in different hippocampal subregions, as
610 well as in non-hippocampal areas involved in fear acquisition (e.g., amygdala, PVT),
611 which in the present study exhibited similar levels of pCREB expression in the OSC and
612 SSC groups. The observation that the dynamics of ERK pathways differ across brain
613 regions involved in fear memory, with peaks occurring at 20 min after a single stimulation
614 in the hippocampus versus 60 min after fear conditioning in the lateral amygdala (Schafe
615 et al., 2000; Di Benedetto et al., 2009; Wang et al., 2014), suggests that the model may
616 be able to predict optimal protocols targeting specific components of fear memory based
617 on the dynamics of intracellular signaling cascades in distinct brain regions. Future
618 studies will test this possibility by modeling the molecular cascades in the lateral
619 amygdala and the medial prefrontal cortex to preferentially target the acquisition and
620 extinction of CS-associated memories, respectively.

621 Our model is an obvious simplification of the mechanisms underlying fear
622 conditioning and extinction. It does not include other molecular cascades critical for LTP
623 and memory formation, due to the lack of empirical data for simulating their dynamics of

activation. For example, calcium/calmodulin-dependent protein kinase II (CaMKII) and protein kinase C (PKC) are also required for LTP induction (Smolen et al., 2020; Malenka et al., 1989; Wang et al., 2016). In addition, we built the model with empirical data of PKA and ERK dynamics from the literature, which are based on *ex vivo* analyses and have limited temporal resolution. Furthermore, the model assumes that the molecular mechanisms for fear memory acquisition are similar to those for extinction. However, despite these limitations, the simplified model using essential biochemical cascades for learning and memory was sufficient to predict enhanced activation of the LTP-related transcription factor CREB in the DG and to facilitate associative learning in three different experiments. A more complex model that incorporates a wider range of intracellular and extracellular processes based on *in vivo* real-time data would likely strengthen the predictive ability of simulations. Further experiments should also investigate the memory enhancing effects of computationally designed training protocols in different types of associative memories, including discrimination learning and backwards conditioning. In addition, it will be important to test whether the effects observed with optimal protocols vary across subjects of different sexes and ages, as well as its efficacy in animal models of cognitive impairment. Together, our results suggest the possibility of using similar model-driven, non-invasive behavioral approaches in preclinical and clinical studies aimed at enhancing learning or restoring memory deficits in humans, as well as to improve extinction-based exposure therapies in patients with anxiety disorders.

MATERIALS AND METHODS

647 **Animals**

648 All experimental procedures were approved by the Center for Laboratory Animal Medicine
649 and Care of The University of Texas Health Science Center at Houston. National
650 Institutes of Health guidelines for the care and use of laboratory animals were strictly
651 followed in order to minimize any potential discomfort and suffering. A total of 120 male
652 Long-Evans hooded adult rats (Charles Rivers Laboratories) 3-5 months of age and
653 weighing 330-450 g were used. Rats were kept in a 12-hour light/12-hour dark cycle with
654 food and water *ad libitum*. Experiments were conducted during the light phase. For the
655 Optimal Extinction experiment, animals were maintained on a restricted diet of 18 g per
656 day of standard laboratory rat chow to increase their motivation during the lever press
657 training. Rats' weights were monitored weekly to make sure that all animals maintained
658 their weight under food restriction.

659

660 **Model Development**

661 The mathematical model for the activation of kinase cascades critical for LTM was
662 modified from a previous model of the signaling cascades for the induction of LTF (Zhang
663 et al., 2011). As mentioned above, the induction of LTM for fear conditioning requires
664 activation of multiple kinase cascades with different temporal dynamics. In the model, the
665 cyclic AMP (cAMP)-PKA pathway is rapidly activated after training, whereas the Raf-
666 MEK-ERK pathway is slowly activated, and both are required for the induction of LTM
667 after fear conditioning and extinction (**Fig. 1A, Fig. 4A**).

668 *PKA Pathway.* The dynamics of cAMP activation upstream of PKA following
669 training and the cAMP-dependent activation of PKA are described by Eqs. 1-4. Inactive

PKA is a holoenzyme (PKA_{RC}, Eq. 2), consisting of regulatory (PKA_R, Eq. 3) and catalytic (PKA_C, Eq. 4) subunits. In response to training, represented by the variable *Stim* in Eq. 1, cAMP is activated (Eq. 1). Active cAMP binds to the regulatory subunit of PKA, leading to the release of free, active catalytic subunit (Fig. 1A) (Eqs. 2-4). '*Stim*' represents the neurotransmitters released by training that activate kinase cascades.

$$\frac{d[cAMP]}{dt} = \lambda \frac{[Stim]}{[Stim] + K_{Stim}} - k_{b,cAMP}[cAMP] \qquad \text{(Eq. 1)}$$

$$\frac{d[PKA_{RC}]}{dt} = k_{b,PKA}[PKA_C][PKA_R] - k_{f,PKA}[PKA_{RC}][cAMP]^2 \qquad \text{(Eq. 2)}$$

$$\frac{d[PKA_R]}{dt} = k_{f,PKA}[PKA_{RC}][cAMP]^2 - k_{b,PKA}[PKA_C][PKA_R] \qquad \text{(Eq. 3)}$$

$$\frac{d[PKA_C]}{dt} = k_{f,PKA}[PKA_{RC}][cAMP]^2 - k_{b,PKA}[PKA_C][PKA_R] \qquad \text{(Eq. 4)}$$

Parameter values are modified from (Zhang et al., 2011) to activate PKA immediately after training, but with PKA activity quickly returning to the basal in ~5 min (Fig. 1B) (Roberson and Sweatt, 1996; Vázquez et al., 2000): λ = 14.6 μM/min, K_{STIM} = 85 μM, $k_{b,cAMP}$ = 4 min^{-1}, $k_{f,PKA}$ = 20 $\mu M^{-2}min^{-1}$, $k_{b,PKA}$ = 12 $\mu M^{-1}min^{-1}$

ERK Pathway. The activation of ERK by training '*Stim*' is via sequential activation of the upstream kinases Raf and MEK (Fig. 1A). Raf activates the MAP kinase kinase MEK, MEK in turn activates the MAP kinase ERK. The differential equations describing the activation of Raf, MEK, and ERK (Eqs. 5-12) are similar to those in (Zhang et al.,

690 2011). However, a discrete time delay in activation of Raf was removed from the
691 phosphorylation of Raf (Eq. 5). Instead, based on empirical data (Wang et al., 2014; Ajay
692 and Bhalla, 2004), parameters describing the activation of Raf were adjusted from (Zhang
693 et al., 2011) so that the ERK activation curve reached the peak around 20 min post-
694 training (Fig. 1B).
695

696 $$\frac{d[Raf^p]}{dt} = k_{f,Raf}[Raf][Stim] - k_{b,Raf}[Raf^p] \quad \text{(Eq. 5)}$$

697 $$[Raf] = [Raf]_{total} - [Raf^p] \quad \text{(Eq. 6)}$$

698 $$\frac{d[MEK]}{dt} = \frac{k_{b,MEK}[MEK^p]}{[MEK^p] + K_{MEK,2}} - \frac{k_{f,MEK}[Raf^p][MEK]}{[MEK] + K_{MEK,1}} \quad \text{(Eq. 7)}$$

699 $$\frac{d[MEK^{pp}]}{dt} = \frac{k_{f,MEK}[Raf^p][MEK^p]}{[MEK^p] + K_{MEK,1}} - \frac{k_{b,MEK}[MEK^{pp}]}{[MEK^{pp}] + K_{MEK,2}} \quad \text{(Eq. 8)}$$

700 $$[MEK^p] = [MEK]_{total} - [MEK] - [MEK^{pp}] \quad \text{(Eq. 9)}$$

701 $$\frac{d[ERK]}{dt} = \frac{k_{b,ERK}[ERK^p]}{[ERK^p] + K_{ERK,2}} - \frac{k_{f,ERK}[MEK^{pp}][ERK]}{[ERK] + K_{ERK,1}} \quad \text{(Eq. 10)}$$

702 $$\frac{d[ERK^{pp}]}{dt} = \frac{k_{f,ERK}[MEK^{pp}][ERK^p]}{[ERK^p] + K_{ERK,1}} - \frac{k_{b,ERK}[ERK^{pp}]}{[ERK^{pp}] + K_{ERK,2}} \quad \text{(Eq. 11)}$$

703 $$[ERK^{p}] = [ERK]_{total} - [ERK] - [ERK^{pp}] \quad \text{(Eq. 12)}$$

704 Parameter values: $k_{f,Raf}$ = 0.001 μM^{-1}min^{-1}, $k_{b,Raf}$ = 0.05 min^{-1}, $[Raf]_{total}$ = 0.5 μM,

705 $k_{f,MEK}$ = 0.41 min^{-1}, $k_{b,MEK}$ = 0.04 μM/min, $K_{MEK,1}$ = 0.20 μM,

706 $K_{MEK,2}$ = 0.19 μM, $[MEK]_{total}$ = 0.5 μM, $k_{f,ERK}$ = 0.41 min^{-1},

707 $k_{b,ERK}$ = 0.12 μM/min, $K_{ERK,1}$ = 0.19 μM,

708 $K_{ERK,2}$ = 0.21 μM, $[ERK]_{total}$ = 0.5 μM.

709 As in (Zhang et al., 2011), a variable '*inducer*' was used to quantify the overlap of

710 activation between PKA and ERK, which together regulate the gene expression

711 necessary for the induction of LTM.

712 $$inducer = k_{inducer}\,[PKA_C]\,[ERK^{pp}] \quad \text{(Eq. 13)}$$

713 where $k_{inducer}$ = 1 μM^{-1}.

714 To determine which protocols could more effectively activate *inducer,* four-trial protocols

715 with three ITIs, each ranging from 2–20 min in steps of 2 min, were simulated. Combining

716 these permutations yielded 1,000 protocols. For each protocol, the maximal (peak)

717 overlap between PKA and ERK was quantified as the peak level of *inducer* produced.

718 Also, the value of *Stim* was varied from 100 to 300 μM to represent weak and strong

719 trainings and to test the robustness of protocols. Based on the maximal overlap, a

720 protocol with ITIs of 8, 8, and 16 min was selected for optimal conditioning and extinction.

721 *Numerical methods.* Fourth-order Runge-Kutta integration was used for

722 integration of all differential equations with a time step of 3 s. Further time step reduction

723 did not lead to significant improvement in accuracy. The steady-state basal levels of

724 variables were determined after at least one simulated day, prior to any manipulations.
725 The model was programmed in XPPAUT (http://www.math.pitt.edu/~bard/xpp/xpp.html)
726 (Ermentrout, 2002) and simulated on Dell Precision T1700 microcomputers.
727
728 **Behavioral Tasks**
729 ***Optimal Conditioning***
730 *Apparatuses*
731 Two distinct chambers (context A and context B) positioned inside sound attenuating
732 boxes were used during the Optimal Conditioning experiments. Context A consisted of a
733 small operant chamber (34 cm high x 25 cm wide x 23 cm deep, 200 lux, Med Associates,
734 see schematic drawing in Fig. 2A top) with one of the two aluminum walls covered by
735 black adhesive paper and two transparent acrylic walls, and a metal grid floor beneath
736 which a microcentrifuge tube (Eppendorf) containing 50 µl of 10% amyl acetate (Sigma-
737 Aldrich) was positioned. Context B consisted of a larger acrylic operant chamber (40 cm
738 high x 50 cm wide x 26 cm deep, 20 lux, Med Associates, see schematic drawing in Fig.
739 2A bottom) with one of its walls covered by a black and white striped paper, and a floor
740 made of a white acrylic board beneath which a microcentrifuge tube (Eppendorf)
741 containing 50 µl of deionized water was positioned.
742
743 *Procedures*
744 On day 0, rats were placed in context A for a 20-min familiarization session. Next, rats
745 were pre-assigned to three experimental groups based on their baseline freezing and
746 locomotor activity during the familiarization session: Regular Conditioning (RC), Short

747 Conditioning (SC), and Optimal Short Conditioning (OSC). On day 1, rats were placed
748 into context A and exposed to one nonreinforced habituation tone (3 kHz, 75 dB, 30 s)
749 followed by distinct fear conditioning protocols (44 min duration). The RC group received
750 eight presentations of a conditioned stimulus (CS, 3 kHz tone, 75 dB, 30 s) that co-
751 terminated with an unconditioned stimulus (US, footshock, 0.7 mA, 0.5 s), with fixed ITIs
752 of 270 s. The SC group received four CS-US pairings with the same ITIs of 270 s, and
753 remained in the chamber until the end of the session. The OSC group received the
754 computationally designed optimal protocol of four CS-US pairings with ITIs of 8, 8, and
755 16 min. On day 2, rats were placed in context B and given two CS presentations (ITI of
756 150 s, 7 min duration) in the absence of US to test the retrieval of tone-associated fear
757 memory in a novel context. On day 3, rats were returned to context A for an extinction
758 training session where they received twelve CS presentations (ITIs of 150 s, 37 min
759 duration). The first four CSs were compared to the last four CSs to assess extinction
760 learning within the same session. On day 4 and 5, rats were placed back in context A and
761 B, respectively, and exposed to an extinction retrieval session (similar to day 2). On day
762 29 and 30, rats were placed back in context A and B, respectively, and exposed to a
763 spontaneous recovery session (similar to day 2). On day 1 and day 2, rats in the same
764 group were trained simultaneously in four chambers with the group order
765 counterbalanced to avoid interference from different protocols in neighboring chambers.
766 On the following days, rats were simultaneously tested in four chambers regardless of the
767 group assignment. Each rat was tested in the exact same chamber across the days.
768 Footshocks, tones, intertrial intervals, and session duration were controlled by an
769 automated video tracking system (ANY-maze, Stoelting), which also quantified the

770 percentage of time freezing, distance traveled, average speed and maximum speed. All
771 rats passed the criteria of 20% of freezing during at least one CS of the fear conditioning
772 session and the first two CSs of the extinction session.
773
774 ***Optimal vs. Spaced Short Conditioning***
775 *Apparatus and Procedures*
776 The same apparatus and contexts described above were used. Following familiarization
777 on Day 0, rats were pre-assigned to two experimental groups based on their baseline
778 freezing and locomotor activity during the familiarization session: Optimal Short
779 Conditioning (OSC) and Spaced Short Conditioning (SSC). The same procedures
780 described above were used here, except that: *i)* the footshock intensity was reduced from
781 0.7 mA to 0.5 mA to decrease the possibility of ceiling effects; *ii)* the SSC group received
782 four CS-US pairings with ITIs of 11 min 10 s. The same automated video tracking system
783 (ANY-maze, Stoelting) described above was used for protocol control and behavioral
784 quantification. One rat that failed the criteria of 20% of freezing during at least one CS of
785 the fear conditioning session and the first two CSs of the extinction session was excluded
786 from the analyses.
787
788 ***Optimal Extinction***
789 *Lever-press training*
790 Rats were placed in an acrylic/aluminum operant chamber (34 cm high x 25 cm wide x
791 23 cm deep, Med Associates, see schematic drawing in Fig. 4A) and trained to press a
792 lever for sucrose on a fixed ratio of one pellet for each press. Next, animals were trained

793 in a variable interval schedule of reinforcement that was gradually reduced across the
794 days (one pellet every 15 s, 30 s, or 60 s) until they reached a minimum criterion of 10
795 presses/min after 7 days of training. All sessions lasted 30 min and were performed on
796 consecutive days. Sucrose pellet delivery, variable intervals, and session duration were
797 controlled by an automated video tracking system (ANY-maze, Stoelting).
798
799 *Apparatus and Procedure*
800 On day 8, rats were placed into the same chamber where they had previously undergone
801 lever presses training. Animals were exposed to five nonreinforced habituation tones (3
802 kHZ, 75 dB, 30 s duration) followed by seven CS-US pairings (ITIs of 150 s, 37 min
803 duration). The footshock intensity was increased from 0.7 mA to 1.0-1.2 mA to result in
804 stronger fear acquisition and consequently higher freezing levels during the extinction
805 training session in the next day. Rats were pre-assigned to three experimental groups
806 based on their freezing and lever presses during the fear conditioning session: Regular
807 Extinction (RE), Short Extinction (SE), and Optimal Short Extinction (OSE). On day 9, rats
808 were returned to the same chamber for a fear extinction session (39 min duration). The
809 RE group received twelve CSs with ITIs of 150 s; the SE group received four CSs with
810 ITIs of 150 s and remained in the chamber until the end of the session; and the OSE
811 group received the computationally designed optimal protocol of four CSs with ITIs of 8,
812 8, and 16 min. On day 10 and 35, rats were placed into the same chamber and received
813 two CSs with an ITI of 150 s to test the strength of fear extinction memory during extinction
814 retrieval and spontaneous recovery tests, respectively. The same automated video
815 tracking system (ANY-maze, Stoelting) described above was used for protocol control

816 and behavioral quantification. Two rats that never reached the criterium of 20% of freezing
817 during at least one CS of the fear conditioning session and the first two CSs of the
818 extinction session were excluded from the analyses.
819
820 **Immunohistochemistry**
821 Rats were perfused with 200 ml of 0.1 M potassium phosphate buffer (KPBS) followed by
822 500 ml of 4% paraformaldehyde (PFA) in 0.1 M sodium phosphate buffer 15 min after day
823 1 of conditioning. Brains were removed from the skull, transferred to a 20% sucrose
824 solution in PFA for 24 h, and stored in a 30% sucrose solution in PFA for another 24 h.
825 Next, coronal brain sections (40 µm thick) were cut with a cryostat (CM1860, Leica) and
826 stored in an antifreeze solution overnight. Sections were blocked in 20% normal goat
827 serum, 0.3% Triton X-100, and 3% hydrogen peroxide in KPBS at room temperature for
828 1 h. Brain sections were then incubated with anti-pCREB serum raised in rabbit (1:1000;
829 EMD Millipore 06-519) overnight at room temperature. After sections were washed with
830 KPBS five times, they were incubated with biotinylated goat anti-rabbit IgG antibody
831 (1:200, Vector Labs, BA-1000-1.5) for 2 h, followed by incubation in ABC kit (1:50, Vector
832 Labs, PK-6100) for 90 min and DAB-Ni solution (Vector Labs, SK-4100) for 25 min.
833 Sections were washed with KPBS and mounted on Superfrost Plus slides. After three
834 days, sections were serially dehydrated with alcohol (Epredia; 50 and 70% for 5min each,
835 95 and 100% for 10 min each) and defatted with Citrisolv (Decon Labs) for 30 min.
836 Sections were then cover-slipped with mounting medium (Permount, Fisher Scientific)
837 before being analyzed microscopically.
838

839 **Microscopy and image analysis**

840 Images were generated with a Nikon microscope (Eclipse NiE Motorized Upright
841 Microscope) equipped with a fluorescent lamp (X-Cite, 120 LED) and a digital camera
842 (Andor Zyla 4.2 PLUS sCMOS). Counts of pCREB-positive cells were performed at 20 x
843 magnification. Cell detection and quantification for the immunohistochemistry experiment
844 were performed automatically using QuPath (Bankhead et al., 2017) by an experimenter
845 blind to the experimental groups. pCREB-positive cell detection was performed using
846 QuPath's optical density sum with a requested pixel size of 0.5 μm. Nucleus parameters
847 included a background radius of 6 μm, median filter radius of 0 μm, sigma of 1.5 μm,
848 minimum area of 2 μm^2, and maximum area of 250 μm^2. Cell expansion was set to 0 μm.
849 Intensity parameters included a threshold of 0.15 and maximum background intensity of
850 5, and intensity threshold parameters were threshold 1 of 0.2, threshold 2 of 0.4, and
851 threshold 3 of 0.6. pCREB-positive cells were automatically counted with a circular region
852 of interest (0.228 mm^2) in each subfield of rat dorsal hippocampus including CA1, CA2,
853 CA3, and DG, as well as in the lateral nucleus of the amygdala (LA), the basal nucleus of
854 the amygdala (BA), the central nucleus of the amygdala (CeA) and the paraventricular
855 nucleus of the thalamus (PVT) according to the rat brain atlas (Paxinos and Watson,
856 2014), and averaged for both hemispheres at 2-3 different antero-posterior levels from -
857 2.4 mm to -4.2 mm from bregma. These brain regions were selected because they have
858 been previously implicated in the acquisition of conditioned fear responses (Herry and
859 Johansen, 2014; Do-Monte et al., 2015). The density of pCREB-positive cells (cells per
860 mm^2) was calculated by dividing the number of pCREB-positive cells by the area of the
861 circular region of interest.

862

863 **Quantification and statistical analysis**

864 Rats were recorded with digital video cameras (Logitech C920) and all behavioral indices
865 were measured using an automated video-tracking system (ANY-maze). Lever presses
866 per minute were calculated by measuring the number of presses during the 30 s cue (or
867 30 s pre-cue) multiplied by two. All graphics and numerical values reported in the figures
868 are presented as mean ± standard error of the mean (SEM). Grubbs' tests (Grubbs, 1969)
869 were used to identify outliers ($p < 0.05$) in each experiment and one rat in Fig. 2 was
870 removed after identification by the test. Shapiro-Wilk tests were performed to determine
871 whether the data have a normal distribution. F tests before pair-wise comparison and
872 Brown-Forsythe tests before multiple group comparison were performed to test if groups
873 have the same variance. Statistical significance for parametric distributions was
874 determined with paired Student's t-test, Welch's t-test, one-way analysis of variance
875 (ANOVA) or two-way repeated-measures ANOVA followed by Tukey post-hoc
876 comparisons, whereas Kruskal-Wallis test followed by Dunn's post-hoc test was used for
877 non-parametric distributions (Software Prism 7), as indicated for each experiment.
878 Sample size was based on estimations from previous literature and experience.

879

880 **Data availability**

881 All data that support the findings presented in this study are available from the
882 corresponding author on reasonable request. Source codes will be submitted to the
883 ModelDB database (McDougal et al., 2015), and to GitHub
884 (https://github.com/Owenxz/Zhang-XO-Enhanced-Learning-2022.git).

885

886

887 **Author Contributions:** X.O.Z, D.S.E., and C.E.C performed and analyzed the behavioral
888 experiments. X.O.Z and C.E.C performed and analyzed the immunohistochemistry
889 experiments. Y.Z. implemented the computational model and ran all simulations. P.S.
890 helped design and implement the computational model. F.H.D-M and J.H.B supervised
891 and contributed to all aspects of this study. All the authors participated in the design of
892 the experiments. X.O.Z. and F.H.D-M interpreted the data and prepared the manuscript
893 with comments from all the co-authors.

894

895 **Acknowledgments:** This work was supported by the Russell and Diana Hawkins Family
896 Foundation Discovery Fellowship and the Dr. John J. Kopchick Fellowship to X.O.Z, NIH
897 grant R01-NS102490 to J.H.B, and NIH grant R00-MH105549, NIH grant R01-MH120136,
898 a Brain & Behavior Research Foundation grant (NARSAD Young Investigator), and a
899 Rising STARs Award from UT System to F.H.D-M. We thank Nikita Watson and Sharon
900 Gordon for their technical and administrative assistance. We also thank current members
901 of the Byrne and Do Monte labs for their valuable comments on the manuscript.

902

903 **REFERENCES**

904 Abel T, Nguyen PV, Barad M, Deuel TA, Kandel ER, Bourtchouladze R (1997) Genetic
905 demonstration of a role for pka in the late phase of ltp and in hippocampus-based
906 long-term memory. Cell 88:615-626.

907 Adams JP, Sweatt JD (2002) Molecular psychology: Roles for the erk map kinase
908 cascade in memory. Annu Rev Pharmacol Toxicol 42:135-163.

909 Ahmed T, Frey JU (2005) Plasticity-specific phosphorylation of camkii, map-kinases and
910 creb during late-ltp in rat hippocampal slices in vitro. Neuropharmacology 49:477-
911 492.

912 Ajay SM, Bhalla US (2004) A role for erkii in synaptic pattern selectivity on the time-
913 scale of minutes. Eur J Neurosci 20:2671-2680.

914 Ajay SM, Bhalla US (2007) A propagating erkii switch forms zones of elevated dendritic
915 activation correlated with plasticity. HFSP J 1:49-66.

916 Alberini CM (2009) Transcription factors in long-term memory and synaptic plasticity.
917 Physiol Rev 89:121-145.

918 Anderson MJ, Jablonski SA, Klimas DB (2008) Spaced initial stimulus familiarization
919 enhances novelty preference in long-evans rats. Behav Processes 78:481-486.

920 Bambah-Mukku D, Travaglia A, Chen DY, Pollonini G, Alberini CM (2014) A positive
921 autoregulatory bdnf feedback loop via c/ebpbeta mediates hippocampal memory
922 consolidation. J Neurosci 34:12547-12559.

923 Bankhead P, Loughrey MB, Fernandez JA, Dombrowski Y, McArt DG, Dunne PD,
924 McQuaid S, Gray RT, Murray LJ, Coleman HG, James JA, Salto-Tellez M,

925 Hamilton PW (2017) Qupath: Open source software for digital pathology image
926 analysis. Scientific reports 7:16878.
927 Barela PB (1999) Theoretical mechanisms underlying the trial-spacing effect in
928 pavlovian fear conditioning. J Exp Psychol Anim Behav Process 25:177.
929 Bartsch D, Ghirardi M, Skehel PA, Karl KA, Herder SP, Chen M, Bailey CH, Kandel ER
930 (1995) Aplysia creb2 represses long-term facilitation: Relief of repression
931 converts transient facilitation into long-term functional and structural change. Cell
932 83:979-992.
933 Bernier BE, Lacagnina AF, Ayoub A, Shue F, Zemelman BV, Krasne FB, Drew MR
934 (2017) Dentate gyrus contributes to retrieval as well as encoding: Evidence from
935 context fear conditioning, recall, and extinction. J Neurosci 37:6359-6371.
936 Bourtchuladze R, Frenguelli B, Blendy J, Cioffi D, Schutz G, Silva AJ (1994) Deficient
937 long-term memory in mice with a targeted mutation of the camp-responsive
938 element-binding protein. Cell 79:59-68.
939 Bouton ME, Maren S, McNally GP (2021) Behavioral and neurobiological mechanisms
940 of pavlovian and instrumental extinction learning. Physiol Rev 101:611-681.
941 Byrne JH, Hawkins RD (2015) Nonassociative learning in invertebrates. Cold Spring
942 Harb Perspect Biol 7.
943 Cain CK, Blouin AM, Barad M (2003) Temporally massed cs presentations generate
944 more fear extinction than spaced presentations. J Exp Psychol Anim Behav
945 Process 29:323-333.
946 Cepeda NJ, Pashler H, Vul E, Wixted JT, Rohrer D (2006) Distributed practice in verbal
947 recall tasks: A review and quantitative synthesis. Psychol Bull 132:354-380.

948 Chaaya N, Jacques A, Belmer A, Beecher K, Ali SA, Chehrehasa F, Battle AR, Johnson
949 LR, Bartlett SE (2019) Contextual fear conditioning alter microglia number and
950 morphology in the rat dorsal hippocampus. Front Cell Neurosci 13:214.
951 Dash PK, Hochner B, Kandel ER (1990) Injection of the camp-responsive element into
952 the nucleus of *aplysia* sensory neurons blocks long-term facilitation. Nature
953 345:718-721.
954 Davis M, Astrachan DI (1978) Conditioned fear and startle magnitude: Effects of
955 different footshock or backshock intensities used in training. J Exp Psychol Anim
956 Behav Process 4:95-103.
957 Davis S, Vanhoutte P, Pages C, Caboche J, Laroche S (2000) The mapk/erk cascade
958 targets both elk-1 and camp response element-binding protein to control long-
959 term potentiation-dependent gene expression in the dentate gyrus in vivo. J
960 Neurosci 20:4563-4572.
961 de Oliveira Alvares L, Do-Monte FH (2021) Understanding the dynamic and destiny of
962 memories. Neurosci Biobehav Rev 125:592-607.
963 Detert JA, Kampa ND, Moyer JR, Jr. (2008) Differential effects of training intertrial
964 interval on acquisition of trace and long-delay fear conditioning in rats. Behav
965 Neurosci 122:1318-1327.
966 Di Benedetto B, Kallnik M, Weisenhorn DM, Falls WA, Wurst W, Holter SM (2009)
967 Activation of erk/mapk in the lateral amygdala of the mouse is required for
968 acquisition of a fear-potentiated startle response. Neuropsychopharmacology
969 34:356-366.

970 Do-Monte FH, Manzano-Nieves G, Quinones-Laracuente K, Ramos-Medina L, Quirk GJ
971 (2015) Revisiting the role of infralimbic cortex in fear extinction with optogenetics.
972 J Neurosci 35:3607-3615.
973 Ermentrout B (2002) Simulating, analyzing, and animating dynamical systems : A guide
974 to xppaut for researchers and students. Philadelphia: Society for Industrial and
975 Applied Mathematics.
976 Fanselow MS (1980) Conditioned and unconditional components of post-shock
977 freezing. Pavlov J Biol Sci 15:177-182.
978 Fanselow MS, LeDoux JE (1999) Why we think plasticity underlying pavlovian fear
979 conditioning occurs in the basolateral amygdala. Neuron 23:229-232.
980 Fernandez SM, Lewis MC, Pechenino AS, Harburger LL, Orr PT, Gresack JE, Schafe
981 GE, Frick KM (2008) Estradiol-induced enhancement of object memory
982 consolidation involves hippocampal extracellular signal-regulated kinase
983 activation and membrane-bound estrogen receptors. J Neurosci 28:8660-8667.
984 Flood JF, Jarvik ME, Bennett EL, Orme AE, Rosenzweig MR (1977) Protein synthesis
985 inhibition and memory for pole jump active avoidance and extinction. Pharmacol
986 Biochem Behav 7:71-77.
987 Genoux D, Haditsch U, Knobloch M, Michalon A, Storm D, Mansuy IM (2002) Protein
988 phosphatase 1 is a molecular constraint on learning and memory. Nature
989 418:970-975.
990 Goldsmith BA, Abrams TW (1991) Reversal of synaptic depression by serotonin at
991 aplysia sensory neuron synapses involves activation of adenylyl cyclase. Proc
992 Natl Acad Sci U S A 88:9021-9025.

993 Goode TD, Maren S (2014) Animal models of fear relapse. ILAR J 55:246-258.
994 Grubbs FE (1969) Procedures for detecting outlying observations in samples.
995 Technometrics 11:1-21.
996 Guan Z, Giustetto M, Lomvardas S, Kim JH, Miniaci MC, Schwartz JH, Thanos D,
997 Kandel ER (2002) Integration of long-term-memory-related synaptic plasticity
998 involves bidirectional regulation of gene expression and chromatin structure. Cell
999 111:483-493.
1000 Herry C, Johansen JP (2014) Encoding of fear learning and memory in distributed
1001 neuronal circuits. Nat Neurosci 17:1644-1654.
1002 Holmes A, Quirk GJ (2010) Pharmacological facilitation of fear extinction and the search
1003 for adjunct treatments for anxiety disorders--the case of yohimbine. Trends
1004 Pharmacol Sci 31:2-7.
1005 Hunsaker MR, Kesner RP (2008) Dissociations across the dorsal-ventral axis of ca3
1006 and ca1 for encoding and retrieval of contextual and auditory-cued fear.
1007 Neurobiol Learn Mem 89:61-69.
1008 Impey S, Obrietan K, Wong ST, Poser S, Yano S, Wayman G, Deloulme JC, Chan G,
1009 Storm DR (1998) Cross talk between erk and pka is required for ca^{2+} stimulation
1010 of creb-dependent transcription and erk nuclear translocation. Neuron 21:869-
1011 883.
1012 Jiang L, Wang L, Yin Y, Huo M, Liu C, Zhou Q, Yu D, Xu L, Mao R (2019) Spaced
1013 training enhances contextual fear memory via activating hippocampal 5-ht2a
1014 receptors. Front Mol Neurosci 12:317.

1015 Johansen JP, Cain CK, Ostroff LE, LeDoux JE (2011) Molecular mechanisms of fear
1016 learning and memory. Cell 147:509-524.
1017 Kandel ER (2001) The molecular biology of memory storage: A dialogue between genes
1018 and synapses. Science 294:1030-1038.
1019 Kheirbek MA, Drew LJ, Burghardt NS, Costantini DO, Tannenholz L, Ahmari SE, Zeng
1020 H, Fenton AA, Hen R (2013) Differential control of learning and anxiety along the
1021 dorsoventral axis of the dentate gyrus. Neuron 77:955-968.
1022 Kida S (2012) A functional role for creb as a positive regulator of memory formation and
1023 ltp. Exp Neurobiol 21:136-140.
1024 Lauterborn JC, Palmer LC, Jia Y, Pham DT, Hou B, Wang W, Trieu BH, Cox CD,
1025 Kantorovich S, Gall CM, Lynch G (2016) Chronic ampakine treatments stimulate
1026 dendritic growth and promote learning in middle-aged rats. J Neurosci 36:1636-
1027 1646.
1028 Liu RY, Cleary LJ, Byrne JH (2011) The requirement for enhanced creb1 expression in
1029 consolidation of long-term synaptic facilitation and long-term excitability in
1030 sensory neurons of *aplysia*. J Neurosci 31:6871-6879.
1031 Lynch G, Cox CD, Gall CM (2014) Pharmacological enhancement of memory or
1032 cognition in normal subjects. Front Syst Neurosci 8:90.
1033 Lynch MA (2004) Long-term potentiation and memory. Physiol Rev 84:87-136.
1034 Malenka RC, Kauer JA, Perkel DJ, Mauk MD, Kelly PT, Nicoll RA, Waxham MN (1989)
1035 An essential role for postsynaptic calmodulin and protein kinase activity in long-
1036 term potentiation. Nature 340:554-557.

1037 Maren S (2005) Synaptic mechanisms of associative memory in the amygdala. Neuron
1038 47:783-786.
1039 Maren S, Phan KL, Liberzon I (2013) The contextual brain: Implications for fear
1040 conditioning, extinction and psychopathology. Nat Rev Neurosci 14:417-428.
1041 Martin KC, Michael D, Rose JC, Barad M, Casadio A, Zhu H, Kandel ER (1997) Map
1042 kinase translocates into the nucleus of the presynaptic cell and is required for
1043 long-term facilitation in *aplysia*. Neuron 18:899-912.
1044 Martin SJ, Grimwood PD, Morris RG (2000) Synaptic plasticity and memory: An
1045 evaluation of the hypothesis. Annu Rev Neurosci 23:649-711.
1046 Mast M, Blanchard RJ, Blanchard DC (1982) The relationship of freezing and response
1047 suppression in a cer situation. The Psychological Record 32:151.
1048 Mayes A, Montaldi D, Migo E (2007) Associative memory and the medial temporal
1049 lobes. Trends Cogn Sci 11:126-135.
1050 McDougal RA, Morse TM, Hines ML, Shepherd GM (2015) Modelview for modeldb:
1051 Online presentation of model structure. Neuroinformatics 13:459-470.
1052 McGaugh JL, Petrinovich LF (1965) Effects of drugs on learning and memory. Int Rev
1053 Neurobiol 8:139-196.
1054 Milner B, Squire LR, Kandel ER (1998) Cognitive neuroscience and the study of
1055 memory. Neuron 20:445-468.
1056 Mohamed HA, Yao W, Fioravante D, Smolen PD, Byrne JH (2005) Camp-response
1057 elements in aplysia creb1, creb2, and ap-uch promoters: Implications for
1058 feedback loops modulating long term memory. The Journal of biological
1059 chemistry 280:27035-27043.

1060 Morgan MA, LeDoux JE (1995) Differential contribution of dorsal and ventral medial
1061 prefrontal cortex to the acquisition and extinction of conditioned fear in rats.
1062 Behav Neurosci 109:681-688.
1063 Muller U, Carew TJ (1998) Serotonin induces temporally and mechanistically distinct
1064 phases of persistent pka activity in *aplysia* sensory neurons. Neuron 21:1423-
1065 1434.
1066 Nakazawa K, Quirk MC, Chitwood RA, Watanabe M, Yeckel MF, Sun LD, Kato A, Carr
1067 CA, Johnston D, Wilson MA, Tonegawa S (2002) Requirement for hippocampal
1068 ca3 nmda receptors in associative memory recall. Science 297:211-218.
1069 Padilla-Coreano N, Do-Monte FH, Quirk GJ (2012) A time-dependent role of midline
1070 thalamic nuclei in the retrieval of fear memory. Neuropharmacology 62:457-463.
1071 Park S, Kramer EE, Mercaldo V, Rashid AJ, Insel N, Frankland PW, Josselyn SA (2016)
1072 Neuronal allocation to a hippocampal engram. Neuropsychopharmacology
1073 41:2987-2993.
1074 Paxinos G, Watson C (2014) Paxino's and watson's the rat brain in stereotaxic
1075 coordinates, Seventh edition. Edition. Amsterdam ; Boston: Elsevier/AP,
1076 Academic Press is an imprint of Elsevier.
1077 Penzo MA, Robert V, Tucciarone J, De Bundel D, Wang M, Van Aelst L, Darvas M,
1078 Parada LF, Palmiter RD, He M, Huang ZJ, Li B (2015) The paraventricular
1079 thalamus controls a central amygdala fear circuit. Nature 519:455-459.
1080 Philips GT, Tzvetkova EI, Carew TJ (2007) Transient mitogen-activated protein kinase
1081 activation is confined to a narrow temporal window required for the induction of
1082 two-trial long-term memory in *aplysia*. J Neurosci 27:13701-13705.

1083 Podlesnik CA, Kelley ME, Jimenez-Gomez C, Bouton ME (2017) Renewed behavior
1084 produced by context change and its implications for treatment maintenance: A
1085 review. J Appl Behav Anal 50:675-697.
1086 Quinn JJ, Wied HM, Ma QD, Tinsley MR, Fanselow MS (2008) Dorsal hippocampus
1087 involvement in delay fear conditioning depends upon the strength of the tone-
1088 footshock association. Hippocampus 18:640-654.
1089 Quirk GJ, Mueller D (2008) Neural mechanisms of extinction learning and retrieval.
1090 Neuropsychopharmacology 33:56-72.
1091 Quirk GJ, Russo GK, Barron JL, Lebron K (2000) The role of ventromedial prefrontal
1092 cortex in the recovery of extinguished fear. J Neurosci 20:6225-6231.
1093 Raman M, McLaughlin K, Violato C, Rostom A, Allard JP, Coderre S (2010) Teaching in
1094 small portions dispersed over time enhances long-term knowledge retention.
1095 Med Teach 32:250-255.
1096 Restivo L, Tafi E, Ammassari-Teule M, Marie H (2009) Viral-mediated expression of a
1097 constitutively active form of creb in hippocampal neurons increases memory.
1098 Hippocampus 19:228-234.
1099 Roberson ED, Sweatt JD (1996) Transient activation of cyclic amp-dependent protein
1100 kinase during hippocampal long-term potentiation. The Journal of biological
1101 chemistry 271:30436-30441.
1102 Roberson ED, English JD, Adams JP, Selcher JC, Kondratick C, Sweatt JD (1999) The
1103 mitogen-activated protein kinase cascade couples pka and pkc to camp
1104 response element binding protein phosphorylation in area ca1 of hippocampus. J
1105 Neurosci 19:4337-4348.

1106 Santini E, Ge H, Ren K, Pena de Ortiz S, Quirk GJ (2004) Consolidation of fear
1107 extinction requires protein synthesis in the medial prefrontal cortex. J Neurosci
1108 24:5704-5710.
1109 Schacher S, Castellucci VF, Kandel ER (1988) Camp evokes long-term facilitation in
1110 *aplysia* sensory neurons that requires new protein synthesis. Science 240:1667-
1111 1669.
1112 Schafe GE, LeDoux JE (2000) Memory consolidation of auditory pavlovian fear
1113 conditioning requires protein synthesis and protein kinase a in the amygdala. J
1114 Neurosci 20:RC96.
1115 Schafe GE, Atkins CM, Swank MW, Bauer EP, Sweatt JD, LeDoux JE (2000) Activation
1116 of erk/map kinase in the amygdala is required for memory consolidation of
1117 pavlovian fear conditioning. J Neurosci 20:8177-8187.
1118 Scharf MT, Woo NH, Lattal KM, Young JZ, Nguyen PV, Abel T (2002) Protein synthesis
1119 is required for the enhancement of long-term potentiation and long-term memory
1120 by spaced training. J Neurophysiol 87:2770-2777.
1121 Selden NR, Everitt BJ, Jarrard LE, Robbins TW (1991) Complementary roles for the
1122 amygdala and hippocampus in aversive conditioning to explicit and contextual
1123 cues. Neuroscience 42:335-350.
1124 Sharif S, Guirguis A, Fergus S, Schifano F (2021) The use and impact of cognitive
1125 enhancers among university students: A systematic review. Brain Sci 11.
1126 Sharma SK, Carew TJ (2004) The roles of mapk cascades in synaptic plasticity and
1127 memory in *aplysia*: Facilitatory effects and inhibitory constraints. Learn Mem
1128 11:373-378.

1129 Sharma SK, Sherff CM, Shobe J, Bagnall MW, Sutton MA, Carew TJ (2003) Differential
1130 role of mitogen-activated protein kinase in three distinct phases of memory for
1131 sensitization in *aplysia*. J Neurosci 23:3899-3907.
1132 Sindreu CB, Scheiner ZS, Storm DR (2007) Ca2+ -stimulated adenylyl cyclases
1133 regulate erk-dependent activation of msk1 during fear conditioning. Neuron
1134 53:79-89.
1135 Smolen P, Zhang Y, Byrne JH (2016) The right time to learn: Mechanisms and
1136 optimization of spaced learning. Nat Rev Neurosci 17:77-88.
1137 Smolen P, Baxter DA, Byrne JH (2020) Comparing theories for the maintenance of late
1138 ltp and long-term memory: Computational analysis of the roles of kinase
1139 feedback pathways and synaptic reactivation. Front Comput Neurosci
1140 14:569349.
1141 Sotres-Bayon F, Sierra-Mercado D, Pardilla-Delgado E, Quirk GJ (2012) Gating of fear
1142 in prelimbic cortex by hippocampal and amygdala inputs. Neuron 76:804-812.
1143 Szapiro G, Vianna MR, McGaugh JL, Medina JH, Izquierdo I (2003) The role of nmda
1144 glutamate receptors, pka, mapk, and camkii in the hippocampus in extinction of
1145 conditioned fear. Hippocampus 13:53-58.
1146 Tao X, Finkbeiner S, Arnold DB, Shaywitz AJ, Greenberg ME (1998) Ca2+ influx
1147 regulates bdnf transcription by a creb family transcription factor-dependent
1148 mechanism. Neuron 20:709-726.
1149 Tronson NC, Schrick C, Fischer A, Sananbenesi F, Pages G, Pouyssegur J, Radulovic
1150 J (2008) Regulatory mechanisms of fear extinction and depression-like behavior.
1151 Neuropsychopharmacology 33:1570-1583.

1152 Vázquez SI, Vázquez A, Peña de Ortiz S (2000) Different hippocampal activity profiles
1153 for pka and pkc in spatial discrimination learning. Behavioral Neuroscience
1154 114:1109-1118.
1155 Verkoeijen PP, Rikers RM, Schmidt HG (2005) Limitations to the spacing effect:
1156 Demonstration of an inverted u-shaped relationship between interrepetition
1157 spacing and free recall. Exp Psychol 52:257-263.
1158 Vossler MR, Yao H, York RD, Pan MG, Rim CS, Stork PJ (1997) Camp activates map
1159 kinase and elk-1 through a b-raf- and rap1-dependent pathway. Cell 89:73-82.
1160 Wang S, Sheng T, Ren S, Tian T, Lu W (2016) Distinct roles of pkcı/λ and pkmζ in the
1161 initiation and maintenance of hippocampal long-term potentiation and memory.
1162 Cell Rep 16:1954-1961.
1163 Wang Y, Zhu G, Briz V, Hsu YT, Bi X, Baudry M (2014) A molecular brake controls the
1164 magnitude of long-term potentiation. Nature communications 5:3051.
1165 Woods AM, Bouton ME (2008) Immediate extinction causes a less durable loss of
1166 performance than delayed extinction following either fear or appetitive
1167 conditioning. Learn Mem 15:909-920.
1168 Zhang Y, Smolen PD, Cleary LJ, Byrne JH (2021) Quantitative description of the
1169 interactions among kinase cascades underlying long-term plasticity of *aplysia*
1170 sensory neurons. Scientific reports 11:14931.
1171 Zhang Y, Liu RY, Heberton GA, Smolen P, Baxter DA, Cleary LJ, Byrne JH (2011)
1172 Computational design of enhanced learning protocols. Nat Neurosci 15:294-297.
1173